

Review

Flexible organic electrochemical transistors for bioelectronics

Zeyu Zhao,¹ Zhiyuan Tian,¹ and Feng Yan^{1,*}

SUMMARY

Flexible organic bioelectronic devices, which extract electronic signals from living systems, have been developed for sensing, recording, and monitoring various physiological states of biological systems. Organic electrochemical transistors (OECTs) have emerged as a promising platform for bioelectronics because of their inherent amplification function, high sensitivity, low cost, easy operation, and compatibility with flexible and wearable devices. This review provides a comprehensive overview of recent advancements in flexible OECTs for biosensing applications, including the fundamental principles and mechanisms of flexible OECTs, various channel materials used for biosensing, functionalization of OECTs for biosensing, use of flexible OECTs for the acquisition of biological signals, bioinformatics analysis of OECT-based biosensors, and development of biomimetic devices. The review concludes with a summary of the state-of-the-art technology for flexible OECT-based biosensors and the future outlook for this rapidly evolving field.

INTRODUCTION

Since Luigi Galvani's series of bioelectric experiments in the 1780s, numerous electronic devices for sensing or stimulating biological signals from living organisms have been developed.^{1–3} Organic bioelectronic devices, which combine electronic signals with living systems,⁴ are widely used to sense, record, and monitor different physiological states of biological systems via electron-ion charge compensation.⁵ Organic bioelectronics encompasses the development and study of organic electronic devices, such as organic optoelectronic devices,⁶ electronic skin,⁷ and organic thin-film transistors (OTFTs).⁸ OTFTs, serving as a crucial component of organic bioelectronics, act as a bridge connecting biology and electronics. Because of their inherent amplifying function, they have emerged as highly advanced biosensing platforms.^{9,10}

Based on the geometrical structure and working mechanism, OTFTs can be classified into three types: organic field-effect transistors (OFETs), electrolyte-gated OFETs (EGOFETs), and organic electrochemical transistors (OECTs). OFETs are three-terminal electronic devices that include source, drain, and gate electrodes, an organic channel, and a dielectric layer. The channel current of OFETs is modulated via field-effect doping between the channel and dielectric layer.¹¹ EGOFETs are enabled by changing the dielectric layer into an electrolyte, creating an electrical double layer at the interface between the electrolyte and channel/gate layers, serving as biosensing areas via a capacitive field-effect mechanism.¹² OECTs share similar device structures with EGOFETs but offer higher transconductance compared to OFETs and EGOFETs due to the doping and de-doping efficacy of ion-permeable channel materials.⁸ Considering the fact that a biological system

¹Department of Applied Physics, The Hong Kong Polytechnic University, Hung Hom, Kowloon, Hong Kong 999077, P.R. China

*Correspondence: apafyan@polyu.edu.hk
<https://doi.org/10.1016/j.xcrp.2023.101673>



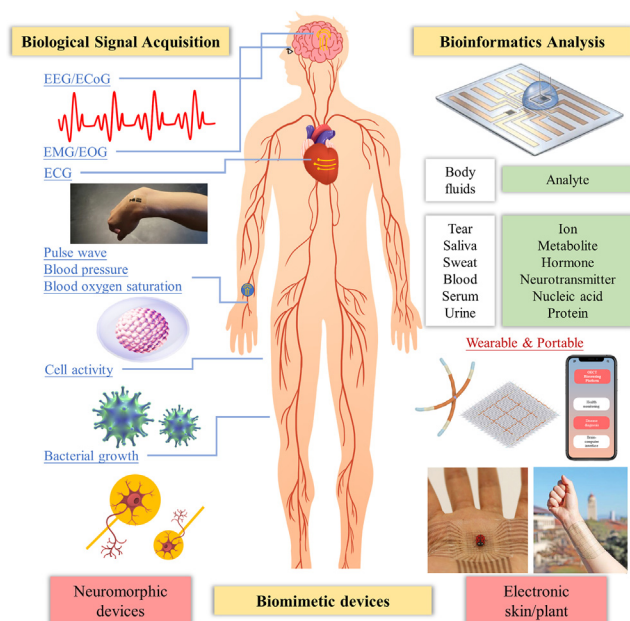


Figure 1. Overview of wide applications of flexible OECTs in biological signal acquisition, bioinformatics analysis, and biomimetic devices

The image of wrist-attached OECTs was reproduced with permission from Dai et al.¹⁸ Copyright 2022, Wiley-VCH. The schematic diagram of OECTs for bioinformatics analysis was reproduced with permission from Wustoni et al.¹⁹ Copyright 2019, Wiley-VCH. The left graphic of electronic skin was reproduced with permission from Wang et al.²⁰ Copyright 2018, Springer Nature; the photograph on the right was reproduced with permission from Zheng et al.²¹ Copyright 2021, AAAS.

contains a high ratio of aqueous solutions, an OECT, a device that only can operate in an electrolyte, is an ideal transducer for biosensing.

Biosensors based on OECTs can be regarded as a combination of signal transduction and amplification for a specific biological system. The carrier density and transmission properties are modulated through various device-analyte interactions, such as hydrogen bonds, charge transfer, dipole-dipole interaction, and reversible transformations.¹³ Stability and biocompatibility of OECTs are crucial requirements as bioelectric devices,¹⁴ and their compatibility with biological systems is mainly evaluated through a series of *in vivo* and *in vitro* experiments. Therefore, OECTs need to be biofunctionalized to obtain stable biosensing functions. Organic mixed ionic-electronic conductors (OMIECs) have emerged as excellent candidates for use in channel materials of OECTs because of their solution processability, flexibility,¹⁵ and biocompatibility.¹⁶ These materials allow for operation in an aqueous environment under low voltages, which results in good sensing interfaces with living organisms.⁸ These features make OECTs a promising platform for the development of highly flexible, sensitive, and stable biosensors in bioelectronics and wearable electronics as well as for the implementation of artificial neuromorphic electronics.¹⁷

In this review, recent advances in the use of flexible OECTs for various biosensing applications are presented (Figure 1). Initially, we introduce the working mechanisms and various p-type and n-type channel materials. We also provide a summary of functionalization techniques for the channel, gate, and electrolyte. Subsequently, we categorize flexible OECT-based biosensors into three major groups: biological signal acquisition, bioinformatics analysis, and biomimetic bioelectronic devices.

We then delve into the functions of each category. Finally, we critically evaluate the perspectives and possible challenges of flexible OECT-based biosensors in practical medical therapy, diagnosis, and commercialization.

MECHANISMS AND CHANNEL MATERIALS OF FLEXIBLE OECTs FOR BIOSENSING

During an OECT sensing process, changes in the effective gate voltage and/or carrier density in the conductive channel brought on by the device-analyte interaction in OECTs cause biological species/signals to modify the device characteristics, typically including channel current (I_{DS}), charge-carrier mobility (μ), threshold voltage (V_{TH}), and current on/off ratio (I_{on}/I_{off}).^{11,22} The materials for channel and gate modifications, especially OMIECs material, take control of the sensing ability. An OECT is a type of organic transistor that typically comprises source, drain, and gate electrodes. The channel through which holes (p-type) or electrons (n-type) flow between the source and drain electrodes is made of an ion-permeable organic semiconductor film. In contrast to OFETs, OECTs employ an electrolyte as the gate insulator instead of a solid-state dielectric layer. During operation, the gate electrode is used to apply a voltage that drives ion injection from the electrolyte into the bulk of the organic channel. This modulation of the doping state and the bulk conductivity of the channel enables OECTs to function as amplifiers, achieving higher transconductance and lower operation voltages.⁸

In 2007, Bernards and Malliaras proposed a physical model for the quantitative prediction of the transconductance (g_m) of OECTs based on parameters, including the channel width (W), length (L), thickness (d), charge-carrier mobility (μ), capacitance per unit volume of the channel (C^*), threshold voltage (V_{TH}), and gate voltage (V_{GS}). The model is represented by²³

$$g_m = \frac{W}{L} \cdot d \cdot \mu \cdot C^* \cdot (V_{TH} - V_{GS}). \quad (\text{Equation 1})$$

The equation for the transconductance of OECTs is similar to that of field-effect transistors, but with the distinction that the product of channel thickness and capacitance per unit volume replaces the capacitance per unit area of the metal-oxide-semiconductor capacitor. This variation enables the channel thickness to be a tunable parameter for the performance of OECTs. Owing to the high capacitance per unit volume of the channel, OECTs exhibit superior amplification performance compared to other transistor technologies when employing volumetric gating with an electrolyte.²⁴

The Bernards model provides valuable insights into the crucial role of carrier mobility and volumetric capacitance in determining the device performance of OECTs. The choice of channel material has a significant impact on both factors, with carrier mobility being responsible for the transport of electronic charges across the channel and volumetric capacitance reflecting the extent of ion penetration, transport, and storage ability of the OMIEC film.²⁵ The penetration and mobility of ions inside the OMIEC film are influenced by their size, charge, and polarity, and these factors can also impact the performance of the device.²⁶ p-Type organic semiconductors are generally preferred over n-type channel materials, due to their higher stability and carrier mobility in aqueous environments. Poly(3,4-ethylenedioxythiophene):polystyrene sulfonate (PEDOT:PSS), conjugated polyelectrolytes (CPEs),²⁷ and glycolated semiconducting polymers¹⁸ are examples of p-type semiconducting polymers used in the production of OECTs for biosensing applications. Among these, PEDOT:PSS is the most extensively investigated semiconducting channel

Table 1. Summary of recently reported OECT-based biosensors for acquisition of biological signals (from 2018 to 2023)

Channel	Device performance	Applications	Reference
PEDOT:PSS	I_{DS} readout resolution: 1 nA	pulse measurement	Tian et al. ²⁹
PEDOT:PSS	LOD: 1.1 Pa; sensitivity: 10,828.2 kPa ⁻¹ ; consumption: <5 μ W	blood pressure measurement	Chen et al. ³⁰
p(g2T-TT)	transconductance: 14 mS; response time: 62 μ s	oxygen saturation detection	Song et al. ³¹
PEDOT:PSS	SNR: 40.02 dB	ECG recordings	Park et al. ³²
PEDOT:PSS	SNR: 24 dB	ECG recordings	Lee et al. ³³
PEDOT:PSS	transconductance: 0.8 mS; response time: 8.3 ms; SNR: 29.0 dB	ECG recordings	Wang et al. ³⁴
PEDOT:PSS	SNR: 52 dB	ECG recordings	Lee et al. ³⁵
Cu3(HHTP)2	volumetric capacitance: 67.8 F cm ⁻³ ; response time: 10 μ s	ECG recordings	Song et al. ³⁶
p(g2T-T)	transconductance: \sim 223 S cm ⁻¹ ; biaxial strain tolerance: 100%	ECG recordings	Dai et al. ¹⁸
h-DPP-g2T	stable ECG recordings at 60% strain	ECG recordings	Chen et al. ³⁷
PEDOT:PSS	response time: 2.9 μ s; SNR: 53.86 dB	EMG/ECG recordings	Cea et al. ³⁸
DPP-g2T	voltage gain: \sim 113	EOG recordings	Yao et al. ³⁹
PEDOT:PSS	response time: 2.6 μ s	EEG recordings	Spyropoulos et al. ⁴⁰
PEDOT: PSS	SNR: \sim 37 dB; response time: 1.42 ms	ECoG recordings	Wu et al. ⁴¹
PEDOT: PSS	3D cell-culture growth; real-time monitoring	cell-culture monitoring	Pitsalidis et al. ⁴²
PEDOT: PSS	real-time monitoring; time resolution: <5 s	cell-vitality monitoring	Decataldo et al. ⁴³
PEDOT: PSS	time response threshold: 1.2 a.u.	cytopathic effect monitoring	Decataldo et al. ⁴⁴
hPSC-CMs	transconductance: \sim 2.5 mS; response time: 100–200 μ s	drug delivery	Gu et al. ⁴⁵
PEDOT:PSS	time resolution: 0.2 Hz	nanomaterial toxicity evaluation	Decataldo et al. ⁴⁶
PEDOT: PSS	transconductance: \sim 20 mS	micro-organ monitoring	Abarkan et al. ⁴⁷
PEDOT: PSS	transconductance: 12 mS V ⁻¹ ; on-to-off current ratios: \sim 105	cell activity/drug delivery/ECG	Liang et al. ⁴⁸
PEDOT: PSS	AC gain: 20.2 dB	single-cell detection	Bonafè et al. ⁴⁹
PEDOT: PSS	cutoff frequencies at -3 dB: 10 kHz	single-cell detection	Hempel et al. ⁵⁰
PEDOT: PSS	LOD: 10 cells μ L ⁻¹	cell-surface glycans	Chen et al. ⁵¹
PEDOT: PSS	transconductance: \sim 2.4 mS	bacterial growth	Frantz et al. ⁵²
PEDOT: PSS	LOD: 880 CFU mL ⁻¹	bacterial growth	Butina et al. ⁵³

layer for OECTs due to its high conductivity, air stability, film-forming property, transparency, and flexibility.

PEDOT:PSS comprises two distinct components. PEDOT functions as the conducting pathway for charge carriers, while PSS serves as a dopant to maintain charge neutrality by compensating for the positive charges (holes) in PEDOT with negatively charged polyanions (PSS⁻). In an OECT that employs PEDOT:PSS, a positive gate voltage is applied to the gate electrode, attracting cations toward the channel, thereby causing them to penetrate the PSS layer and enter the PEDOT layer. The cations compensate for the anionic charges in the PSS layer, resulting in a reduction in the density of holes in the PEDOT layer. This reduction in hole density decreases the channel current, resulting in the device operating in depletion mode. The magnitude of the current modulation is proportional to the gate voltage, allowing for the sensitive detection of analytes that influence the gate potential. Various channel materials used in OECTs for different applications are presented in [Tables 1 and 2](#), while a more comprehensive overview of both p-type and n-type channel materials can be found in our previous review.²⁸

FUNCTIONALIZATION OF OECTs FOR BIOSENSING

Channel functionalization

OECT channels can be conveniently functionalized with biomolecules for biosensing through various physical interactions, such as electrostatic interactions

Table 2. Summary of recently reported biosensors based on OECTs for bioinformatics analysis (from 2018 to 2023)

Applications	Channel	LOD	Analyte	Reference
Ion sensors	PEDOT:PSS	0.1 mM/0.1 mM	Ca ²⁺ /glucose	Lin et al. ⁵⁴
	PEDOT:PSS	0.1 mM	cations	Kim et al. ⁵⁵
	PEDOT:PSS	0.75 mM/0.80 mM	Na ⁺ /K ⁺	Li et al. ⁵⁶
	PEDOT:PSS	–	H ⁺ /HCO ₃ [–]	Chen et al. ⁵⁷
	PEDOT:PSS	10 μM	NO ₃ [–]	Takemoto et al. ⁵⁸
Metabolite sensors	P-90	10 nM	glucose	Ohayon et al. ⁵⁹
	P-90	1 nM	glucose	Koklu et al. ⁶⁰
	PEDOT:PSS	30 nM/30 nM/100 nM	glucose/dopamine/uric acid	Yang et al. ⁶¹
	PEDOT:PSS	100 nM/100 nM/5 nM	glucose/glutamate/dopamine	Wu et al. ⁶²
	PEDOT:PSS	10 nM	glucose	Qing et al. ⁶³
	PEDOT:PSS	–	glucose	Diacci et al. ⁶⁴
	P-90	10 μM	lactate	Pappa et al. ⁶⁵
	polypyrrole	1 nM	lactate	Zhang et al. ⁶⁶
	PEDOT:PSS	10 nM	ascorbic acid	Zhang et al. ⁶⁷
	PEDOT:PSS	1 nM	sialic acid	Zhu et al. ⁶⁸
	PEDOT:PSS	4.5 μM	uric acid	Galliani et al. ⁶⁹
	PEDOT:PSS	8.8 ag mL ^{–1}	cortisol	Aerathupalathu Janardhanan et al. ⁷⁰
Hormone sensors	PEDOT:PSS	1 pg mL ^{–1}	cortisol	Parlak et al. ⁷¹
	PEDOT:PSS	100 pM	cortisol	Demuru et al. ⁷²
	PEDOT:PAH1	5 μM	acetylcholine	Fenoy et al. ⁷³
Neurotransmitter sensors	PEDOT:PSS	5 nM	dopamine	Li et al. ⁷⁴
	PEDOT:PSS	30 nM	dopamine	Xie et al. ⁷⁵
	PEDOT:PSS	90 pM	epinephrine	Saraf et al. ⁷⁶
	PEDOT:PSS	1 fM	DNA	Song et al. ⁷⁷
Nucleic acid	PEDOT:PSS	100 fM	DNA	Sensi et al. ⁷⁸
	PEDOT:PSS	1 pM	miRNA17	Gao et al. ⁷⁹
	PEDOT:PSS	2 pM	miRNA21	Peng et al. ⁸⁰
	PEDOT:PSS	10 fM	miRNA21	Fu et al. ⁸¹
	PEDOT:PSS	–	SARS-CoV-2 neutralizing antibodies	Decataldo et al. ⁴⁴
Protein sensors	p(gOT2-g6T2)	1.2 zM	SARS-CoV-2 and MERS-CoV spike proteins	Guo et al. ⁸²
	PEDOT:PSS	1 fM	COVID-19 IgG	Liu et al. ⁸³
	PEDOT:PSS	550 pg mL ^{–1}	tear lysozyme	Li et al. ⁸⁴
	PEDOT:PSS	50 fg mL ^{–1}	human IgG	Hu et al. ⁸⁵
	PEDOT:PSS	0.025 HAU	human influenza virus	Hai et al. ⁸⁶
	p(C6NDI-T)	100 aM	SARS-CoV-2 spike protein	Koklu et al. ⁸⁷
	PEDOT:PSS	0.1 pM	caspase-3	Yu et al. ⁸⁸
	PEDOT:PSS	2 nM	α-amino acids	Zhang et al. ⁸⁹
	p(gOT2-g6T2)	2.21 fM	amyloid-β	Koklu et al. ⁹⁰
	P3HT	7 zM	human IgG	Song et al. ⁹¹
	PT-COOH	10 fg mL ^{–1}	SARS-CoV-2 antibody	Song et al. ⁹²

and physical absorption. For instance, adjusting the pH value of the acetylcholinesterase solution to 7.4 facilitated its direct electrostatic anchoring onto the OECT channel (Figure 2A).⁷³ In addition, enzymes such as lactate oxidase (LOx) and glucose oxidase (GOx) have been demonstrated to adhere to the top of channel area through physical adsorption.^{59,60,65} Notably, the n-type copolymer P-90 channel material possesses hydrophilic glycol side chains that can enhance enzyme conjugation, making it an attractive substrate for enzyme immobilization.⁶⁵ P-90/enzyme composites not only serve as channel materials but can also be immobilized on gate electrodes, as shown in the Figure 2B. When GOx consumes glucose on the channel area or gate electrode, the sensor is triggered and can detect glucose directly without the need for external mediators, as it does not rely on H₂O₂ catalysis.⁶⁰

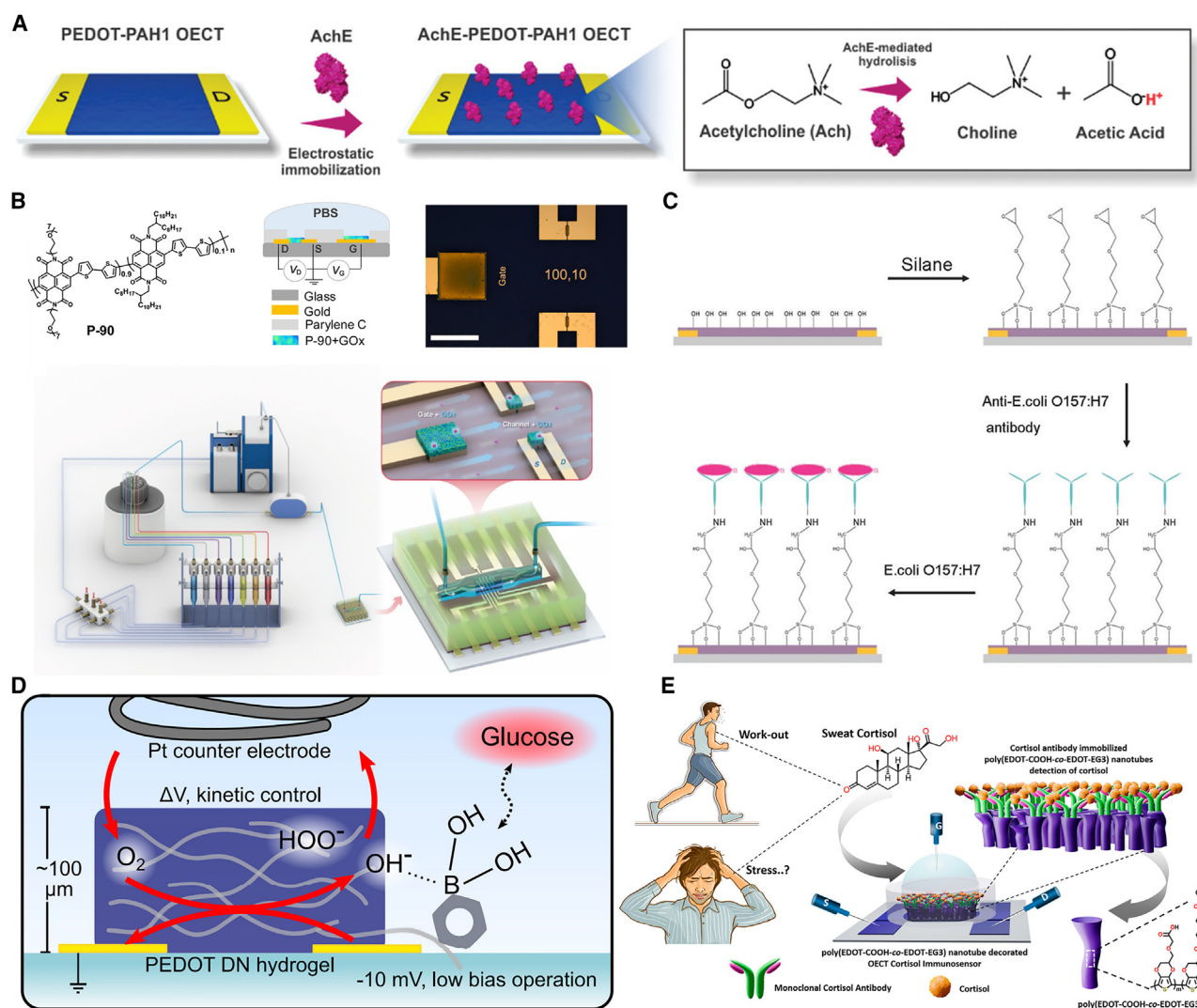


Figure 2. Typical channel functionalization of OECTs

(A) Schematic of the electrostatic immobilization of acetylcholinesterase on the channel of a PEDOT-PAH1-based OECT. Reproduced with permission from Fenoy et al.⁷³ Copyright 2021, Wiley-VCH.

(B) Schematic of P-90 material, the construction of an OECT, and a microfluidic integrated OECT system with perfusion. Reproduced with permission from Koklu et al.⁶⁰ Copyright 2021, Elsevier.

(C) Schematic of anti-*E. coli* O157:H7 antibodies and *E. coli* O157:H7 bacteria immobilized and captured on the top of PEDOT:PSS layer of an OECT. Reproduced with permission from He et al.⁹³ Copyright 2012, Royal Society of Chemistry.

(D) Scheme of double-network hydrogel channel layer comprising PBA and PEDOT:PSS for glucose monitoring. Reproduced with permission from Tseng and Sakata.⁹⁴ Copyright 2022, American Chemical Society.

(E) Schematic of cortisol antibodies modified on the channel of an OECT decorated with poly(EDOT-COOH-co-EDOT-EG3) nanotubes, for human stress detection. Reproduced with permission from Aerathupalathu Janardhanan et al.⁷⁰ Copyright 2022, American Chemical Society.

The immobilization of biorecognition elements onto organic channels can be effectively achieved through chemical immobilization techniques. In 2012, we utilized silane to immobilize anti-*E. coli* O157:H7 antibodies onto the surface of a PEDOT:PSS channel (Figure 2C), resulting in the development of an OECT-based bacterial sensor that allows for the disposable detection of *E. coli* O157:H7 bacteria.⁹³ Another promising approach involves the use of a bilayer channel structure as a sensing layer. By incorporating phenylboronic acid (PBA) into PEDOT:PSS, diol-based binding sites are created for glucose detection, exhibiting stability for

a continuous month of immersion (Figure 2D). The hydrogel structure of OECTs enables efficient switching (on/off ratios of 10^3) and adequate transconductances ($g_m \sim 40 \text{ mS}$), allowing them to operate within the linear regime. This property permits the optimization of device response to electrochemical signals at the lowest applied potentials, which is a crucial advantage for the progression of bioelectronic interfaces.⁹⁴ Similarly, a channel chemical modification involving a PEDOT:PSS underlayer and a poly(EDOT-COOH-co-EDOT-EG3) nanotube-decorated upper layer has been used to provide a carboxyl acid side chain for coupling with cortisol antibodies (Figure 2E). The resulting OECTs exhibited high reproducibility, stability, sensitivity, and selectivity for the detection of cortisol in artificial sweat, with a limit of detection (LOD) of $0.0088 \text{ fg mL}^{-1}$. These characteristics make the sensor clinically practical and promising for detecting human stress.⁷⁰

The biocompatibility of OMIECs allows for the *in situ* cultivation and monitoring of cells or tissues directly on their surfaces, which is particularly useful for detecting cellular physiological activities. For instance, OECTs with cell-modified channels have been utilized to monitor the real-time adhesion and growth of cells⁴² as well as to monitor the activation and inhibition of cells.⁹⁵ Moreover, *in situ* cell-modified channel-modification techniques have been used for real-time monitoring of cellular vitality,⁴³ *in vitro* monitoring cell activities,⁹⁶ cell toxicity,⁴⁶ and cytopathic effects.⁴⁴ Further details on these applications are provided in the section “cell activity.”

Gate functionalization

Gate functionalization is a popular strategy for developing OECT-based biosensors because gate modification is channel independent, and biorecognition events occurring on the gate working electrode can cause significant changes in the channel's behavior due to the high transconductance of OECTs. Various biorecognition elements, such as proteins, enzymes, and nucleic acids, have been modified on the gate surface of OECTs to achieve specific antibody-antigen recognition, enzyme catalysis, and DNA/RNA capture. These reactions induce electron transfer and potential changes. Moreover, when considering real measurements, sensitivity, selectivity, and stability of OECTs must be taken into account, leading to potential gate modification of other functional materials such as self-assembled monolayers (SAMs), nanomaterials, selectively permeable membranes, charged membranes, and encapsulation layers.

To enhance the binding of biorecognition elements, such as DNA, RNA, and amino-glycoside aptamers, onto the gate surface of OECTs, the modification of SAMs is typically carried out prior to the modification of biorecognition elements because these biorecognition elements may not readily bind directly onto the gate surface. Thiol-modified bioprobes are commonly used as intermediates as a chemical SAM to facilitate the binding of biorecognition elements onto the gate surface.^{82,97,98} In the specific case of detecting tobramycin, thiolated aptamers were immobilized onto a gold electrode of OECTs to improve binding onto the gate surface. By placing the Au electrodes in thiolated aptamers for several hours, an Au-thiolated bond was formed (Figure 3A), resulting in higher current modulation across the transistor channel compared to traditional electrochemical aptamer-based sensors.⁹⁸ Furthermore, the OECT-based sensor maintained stable current output even when the device was miniaturized, demonstrating its potential for use in non-invasive and spatial-resolution biosensing applications. Similarly, functional modification of biological SAMs provides an ideal immobilization environment for various types of biomolecules, including nucleic acids,^{97,77} antibodies,^{82,99} antigens,⁸³ and enzymes,^{61,100,101} using biological SAMs. In the development of the OECT-based

antigens biosensors, both chemical and biological SAM modifications have been employed as shown in Figure 3B.⁸² A chemically modified SpyTag peptide was immobilized on the top of the Au gate electrode to capture the nanobody-SpyCatcher fusion protein. This biofunctionalization approach mitigates the risk of functional loss of proteins, such as nanobody or SpyCatcher, due to direct chemical modification, resulting in sensors with single-molecule sensitivity.

The use of nanomaterials, such as metal nanoparticles, has been a widely used approach to enhance the sensitivity of OECTs by modifying the surface of gate electrodes. In a study conducted by our group in 2011, platinum nanoparticles (Pt NPs) were employed to modify the gate electrodes of OECTs, resulting in highly sensitive glucose monitoring with a detection limit of 5 nM (Figure 3C).¹⁰¹ Additionally, carbon-based materials, including multi-wall carbon nanotubes (MWCNTs), graphene, graphene oxide, and reduced graphene oxide, have been found to facilitate enzyme immobilization. This is due to the presence of oxygen-containing functional groups and larger surface area, which provide more sites for enzyme attachment.^{100,101,103}

Selectively permeable membranes and charged membranes have been utilized to enhance the selectivity of OECTs. For instance, a 3,4-ethylenedioxythiophene-based Na⁺ and K⁺ ion-selective membrane (ISM) was deposited on top of an OECT gate, achieving dual cation detection for the first time (Figure 3D).¹⁹ ISMs provide a direct and efficient approach for large-scale production and adaptation into various geometries for detecting alkali-metal ions in both *in vivo* and *in vitro* settings. Recently, cortisol-selective membranes were fabricated using molecularly imprinted polymers and interposed between gate electrode and channel, achieving sweat cortisol detection with a linear detection range of 0.01–10.0 μM and high selectivity against cortisol's structural analogs (Figure 3E).⁷¹ Charged membranes, on the other hand, have been shown to effectively block the diffusion of electro-active substances on the gate surface of OECTs. Liao et al. utilized Nafion and polyaniline as charged membrane to repel the negatively and positively charged molecules, respectively.¹⁰⁰ Nafion, a polymer with a stable Teflon backbone and containing acidic sulfonic groups, possesses a negative charge, which enables it to block the diffusion of anionic electro-active substances, such as ascorbic acid and uric acid, through electrostatic interactions. Conversely, polyaniline doped with an acidic dopant takes on a positive charge due to the presence of protonated amine groups, and it effectively repels the positively charged molecules, such as dopamine, in biosensing applications.

Encapsulation layers are typically applied as the final step of gate functionalization to immobilize the functional layer. Chitosan is commonly utilized as an encapsulation layer on the OECT gate, either alone or in combination with other biomolecules, due to its biocompatibility, biodegradability, excellent film-forming ability, high water permeability, and mucoadhesive properties.^{100,101} Pappa et al. employed a chitosan/ferrocene/enzyme mixed solution, drop-casted onto the glycidoxypentyltrimethoxysilane deposited gate electrode to achieve multi-analyte saliva testing, as illustrated in Figure 3F.¹⁰² Another effective choice for gate electrode encapsulation to prevent non-specific bindings is bovine serum albumin (BSA).^{83,62}

Electrolyte functionalization

Biorecognition events typically occur in the electrolyte solution that covers the semi-conducting channel and gate electrode of OECTs. Therefore, analytes such as metabolites, nucleic acid, hormone, and protein are added into the aqueous electrolyte. Similarly to the functionalization of the channel and gate, biorecognition

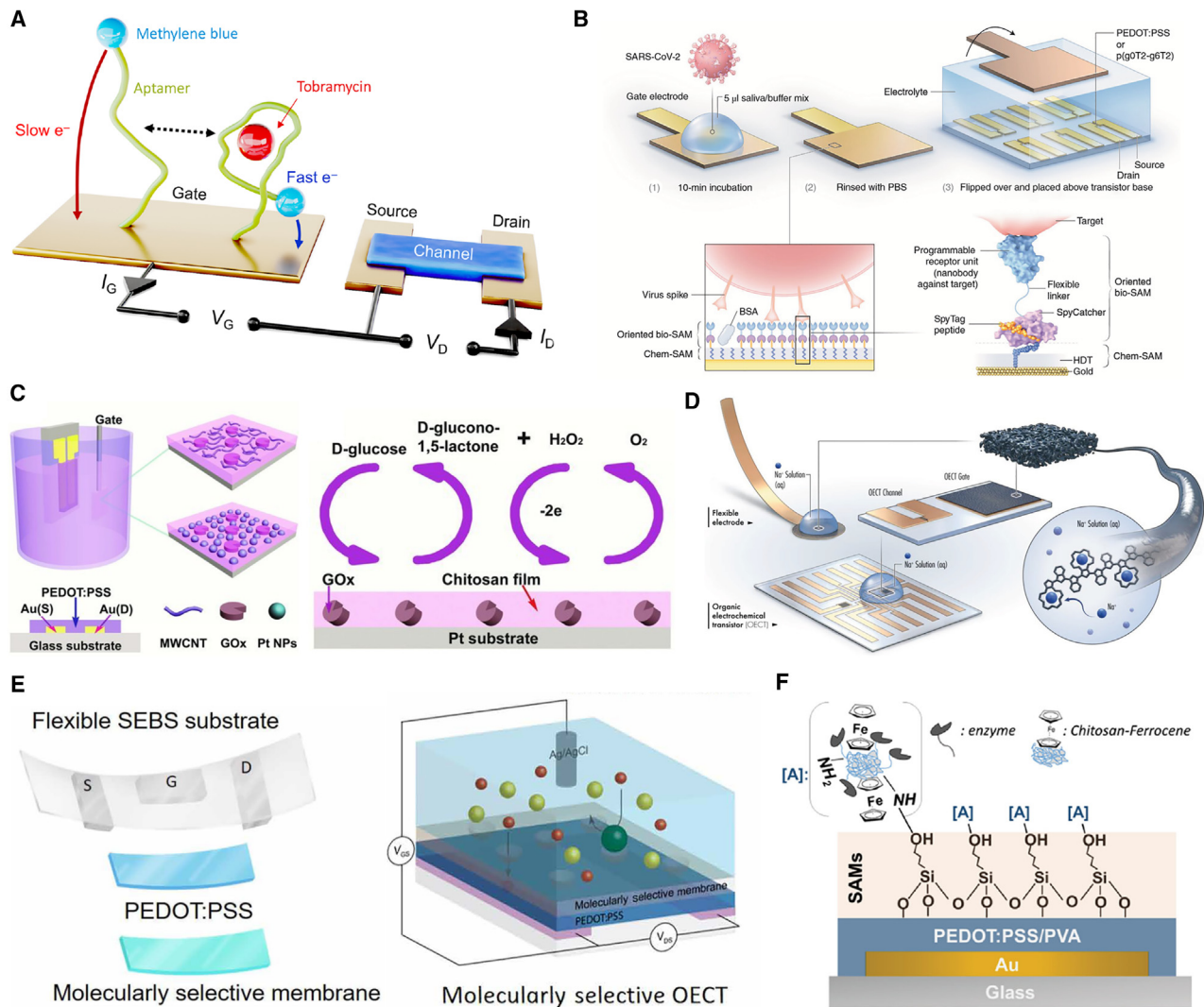


Figure 3. Typical gate functionalization of OECTs

(A) Schematic of the immobilization of thiolated aptamers onto a gold electrode of OECTs. Reproduced with permission from Biding et al.⁹⁸ Copyright 2022, AAAS.

(B) Schematic of nanobody-modified OECT sensor, which includes chemical and biological SAM functionalizations. Reproduced with permission from Guo et al.⁸² Copyright 2021, Springer Nature.

(C) Schematic of a multi-layer gate-modification approach for glucose OECT biosensing, which comprises MWCNTs, GOx, Pt NPs, and chitosan modifications on the Pt gate electrodes. Reproduced with permission from Tang et al.¹⁰¹ Copyright 2011, Wiley-VCH.

(D) Schematic of an OECT based on PEDOT, with a Na⁺ and K⁺ ion-selective membrane deposited on top of gate electrode. Reproduced with permission from Wustoni et al.¹⁹ Copyright 2019, Wiley-VCH.

(E) Schematic of a flexible OECT on an elastic SEBS substrate, with a PEDOT:PSS semiconducting layer and a molecularly selective membrane. Reproduced with permission from Parlak et al.⁷¹ Copyright 2018, AAAS.

(F) Schematic of gate biofunctionalization using a mixed solution of PEDOT:PSS/PVA and chitosan/ferrocene/enzyme. Reproduced with permission from Pappa et al.¹⁰² Copyright 2016, Wiley-VCH.

elements can be directly incorporated into the aqueous electrolyte or ionic liquid to form a gel-format or solid-state electrolyte.^{104,30} Scheiblin et al. demonstrated the development of a solid-state electrolyte for lactate detection by incorporating *N*-isopropylacrylamide (NIPAAm), *N,N'*-methylene-bis(acrylamide) (MBAAm), and LOx.¹⁰⁵ This approach offers an advantage over liquid electrolytes, as it overcomes the problem of aqueous leakage and contamination that can arise during liquid

handling in biosensing applications. Additionally, all-solid-state OECTs are well suited for stress sensing because of their skin-attachment performance. This approach has been widely used to detect physiological signals, including pulse wave²⁹ and blood pressure,³⁰ among others, as summarized in the following section.

BIOLOGICAL SIGNAL ACQUISITION

Biological signals recognition, such as wrist pulse, blood pressure, electrophysiological process, nerve impulse, and cell activity, is of great significance to understanding the laws of human life, finding differences between individuals, exploring the prevention and diagnosis of diseases, and developing instruments for precision medicine. OECTs have been extensively used in biological signal acquisition owing to their intrinsic flexibility, signal amplification, and low-cost processing. In this section, we aim to present a comprehensive overview of the most recent advancements in OECT-based biosensors that are utilized for the acquisition of diverse biological signals. Our discussion will be supported by [Table 1](#), which provides a summary of the significant findings in this field.

Physiological information

OECTs have been used to monitor dynamic changes in active human organs such as blood vessels, skin, and heart, providing valuable physiological information including pulse wave,²⁹ blood pressure,³⁰ oxygen saturation,³¹ and organ signals.^{47,48} Physical signals, such as pressure, are commonly detected using OECT-based sensors, where a solid-state electrolyte is used to bridge the semiconducting channel and the gate electrode instead of a solution electrolyte. Chen et al. demonstrated the integration of a microstructured solid electrolyte to fabricate an ultra-flexible all-solid-state OECT that modulates through a pressure-sensitive ionic doping process, offering the potential for measuring human blood pressure.³⁰ As shown in [Figure 4A](#), pressure maps clearly distinguish different-shaped patterns placed on the OECT array. Similarly, Tian et al. developed a coin-sized OECT with a solid-state ion gel as electrolyte, allowing for self-calibration and personalized pulse-wave measurements ([Figure 4B](#)).²⁹ Alternatively, an elastic well can be used to confine aqueous solutions as an electrolyte in OECT-based pressure sensors.¹⁰⁶

In addition to pressure sensors, photoplethysmogram (PPG) sensors are frequently employed for the dynamic analysis of physiological signals, which are typically composed of a light source (such as a light-emitting diode [LED]) and a photodetector (such as photodiodes and phototransistors) placed on the skin surface.¹⁰⁷ Recent advancements have integrated an OECT with a photodiode module to unlock the potential of a photodiode for acquiring physiological signals.¹⁰⁸ However, the complicated integration of LEDs in PPG sensors increase their power consumption. To address this issue, our group has developed a novel flexible perovskite solar cell (PSC) gated OECT for PPG sensing ([Figure 4C](#)), which operates at an ultra-low working voltage of -1 mV, enabling an ultra-low electrical power consumption of approximately 8.8 nW.³¹ These devices can be placed on the surface of the human body to monitor PPG signals under ambient light or remotely operated at a distance of up to 10 mm, as shown in [Figure 4C](#). Furthermore, by integrating with optical filters, these devices can continuously track peripheral oxygen saturation.

Electrophysiological process

OECT-based biosensors offer a crucial capability of monitoring the electrophysiological process, as they can directly interface with muscular tissue, nerve fibers, or brain circuits to detect various electrophysiological signals such as electrocardiographic (ECG),^{18,32–37,109} muscle tissue electromyographic (EMG),^{110,38} electro-oculographic

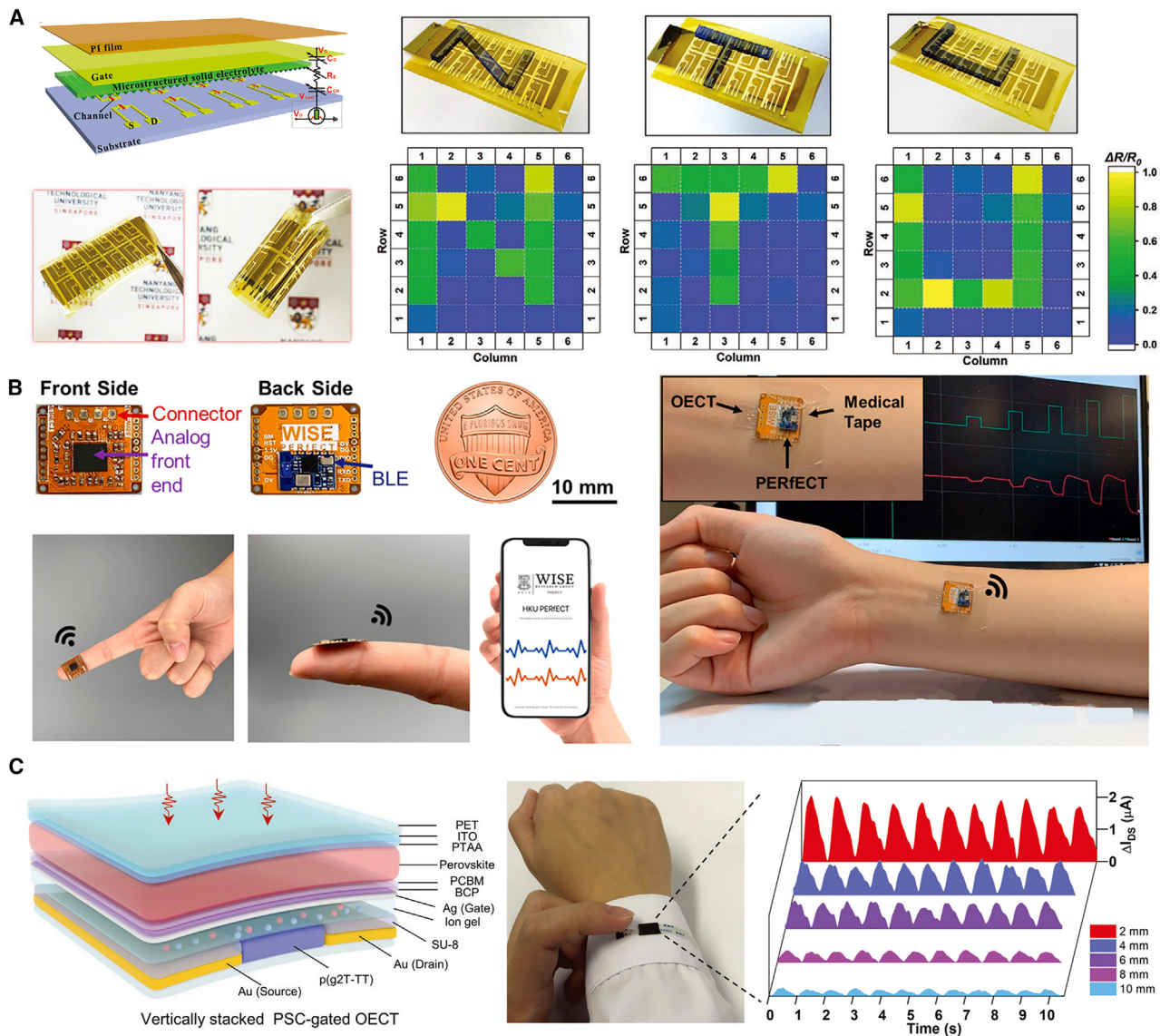


Figure 4. Acquisition of physiological information using OECT-based biosensors

(A) Schematic and photography of an ultra-flexible all-solid-state OECT, and pressure mapping images of different-shaped patterns placed on an array of OECTs. Reproduced with permission from Chen et al.³⁰ Copyright 2020, Wiley-VCH.

(B) Design of a coin-sized OECT system attached onto human skin and measured by a smartphone. Reproduced with permission from Tian et al.²⁹ Copyright 2022, American Chemical Society.

(C) Schematic structure of a PSC gated OECT and images of PPG signals recorded remotely at different distances between fingers and the device. Reproduced with permission from Song et al.³¹ Copyright 2023, Wiley-VCH.

(EOG),³⁹ electroencephalographic (EEG),^{40,111,112} and electrocorticographic (ECoG) recordings,¹¹³ and mapping of brain activity.⁴¹ Typically, a flexible thin-film device is attached directly onto the skin, such as forearm, chest, and wrist,^{109,114,115} or directly onto the heart to measure the ECG signals.³² Despite recent advancements, long-term monitoring of wearable functional electronic devices remains challenging due to the instability of integrated power sources under mechanical deformation. Park et al. have addressed this issue by developing ultra-flexible self-powered OECT-based biosensors that integrate a double-grating-patterned organic photovoltaic device.³² This was achieved through the employment of a high-throughput room-temperature

molding process, which created nanogating morphologies on the charge-transporting layers with a periodicity of 760 nm. The resulting biosensors offer stable ECG monitoring capabilities, making them highly suitable not only for long-term and continuous monitoring of ECG signals attached to the human finger but also to the heart of a rat (Figure 5A). However, ECG signals have a low amplitude (\sim mV) and require amplification and downstream processing. The integrity of these signals can also be easily degraded by surrounding interferences, making continuous monitoring of ECG waves challenging. To address this issue, an innovative approach has been developed to enhance the durability and comfort of OECTs attached to human skin by using a non-volatile ion-gel electrolyte, allowing for continuous monitoring of ECG signals for more than 3 h with reusability for more than a week (Figure 5B).³³ Efforts have also been devoted to improving the gas permeability of OECT-based ECG sensors by developing a fibrous nanomesh OECT with gas-permeable porous solid-state polymer electrolyte, which has demonstrated the ability to record long-term and high-quality ECG signals.³⁴

Wearable ECG mapping is a valuable approach for obtaining comprehensive information on the heart's electrical activity for diagnosis, as it involves recording ECG signals from different perspectives. However, this technique can pose challenges, as it requires large-scale uniform sensor matrices with high sensitivity. To address this issue, ultra-flexible 4×4 OECT arrays were manufactured on a honeycomb grid substrate to provide high spatial and temporal resolutions for monitoring the moving hearts of rats (Figure 5C).³⁵ Impressively, poly(3-methoxypropyl acrylate) was coated on the OECT arrays to achieve non-thrombogenicity and enable ECG monitoring even with capillary bleeding. The ECG signals obtained from these arrays showed a high signal-to-noise ratio (SNR) of 52 dB, indicating the accurate and reliable recording of electrophysiological signals. Recently, our group also made a significant breakthrough in the field of on-skin ECG mapping by utilizing ultra-thin flexible OECT arrays based on highly oriented $\text{Cu}_3(\text{HHTP})_2$, a type of 2D conjugated metal-organic framework (c-MOF), as the channel materials.³⁶ The ion-conductive vertical nanopores formed within the $\text{Cu}_3(\text{HHTP})_2$ films were found to facilitate efficient ion transport in the bulk and enable high volumetric capacitance, resulting in fast response speeds and ultra-high transconductance. An ultra-thin flexible, large-area, and operationally stable device array with high yield and uniformity on a polyimide substrate was developed and conformally attached to the human chest for monitoring ECG signals from different angles (Figure 5D).³⁶ The device array provided various waveforms that were comparable to those obtained from multi-lead ECG measurements, while also being wearable and convenient for the patient. This innovation has the potential to significantly improve the diagnosis and treatment of various medical conditions related to the heart's electrical activity.

Intrinsically stretchable redox-active semiconducting polymers poly(2-(3,3'-bis(2-(2-methoxyethoxy)ethoxy)ethoxy)-[2,2'-bithiophen]-5)yl thiophene) (p(g2T-T)) were reported as the channel layer of OECT devices. The p(g2T-T) polymers showed exceptional stretchability, withstanding 200% strain and 5,000 repeated stretching cycles at 100% without any crack formation or performance degradation. The stretchable OECTs were attached onto a human wrist to measure ECG recordings, and the results exhibited stable recordings during joint movements and skin deformation (Figure 5E).¹⁸ More recently, Chen et al. reported a material-level design concept to fabricate highly stretchable OECTs using an intrinsically stretchable organic semiconductor film with a honeycomb porous structure as a pre-stretched platform (phs-h-DPP-g2T) to record ECG signals under various strains (Figure 5F).³⁷ In the typical stretchable OECT fabrication, h-DPP-g2T was spin-coated on

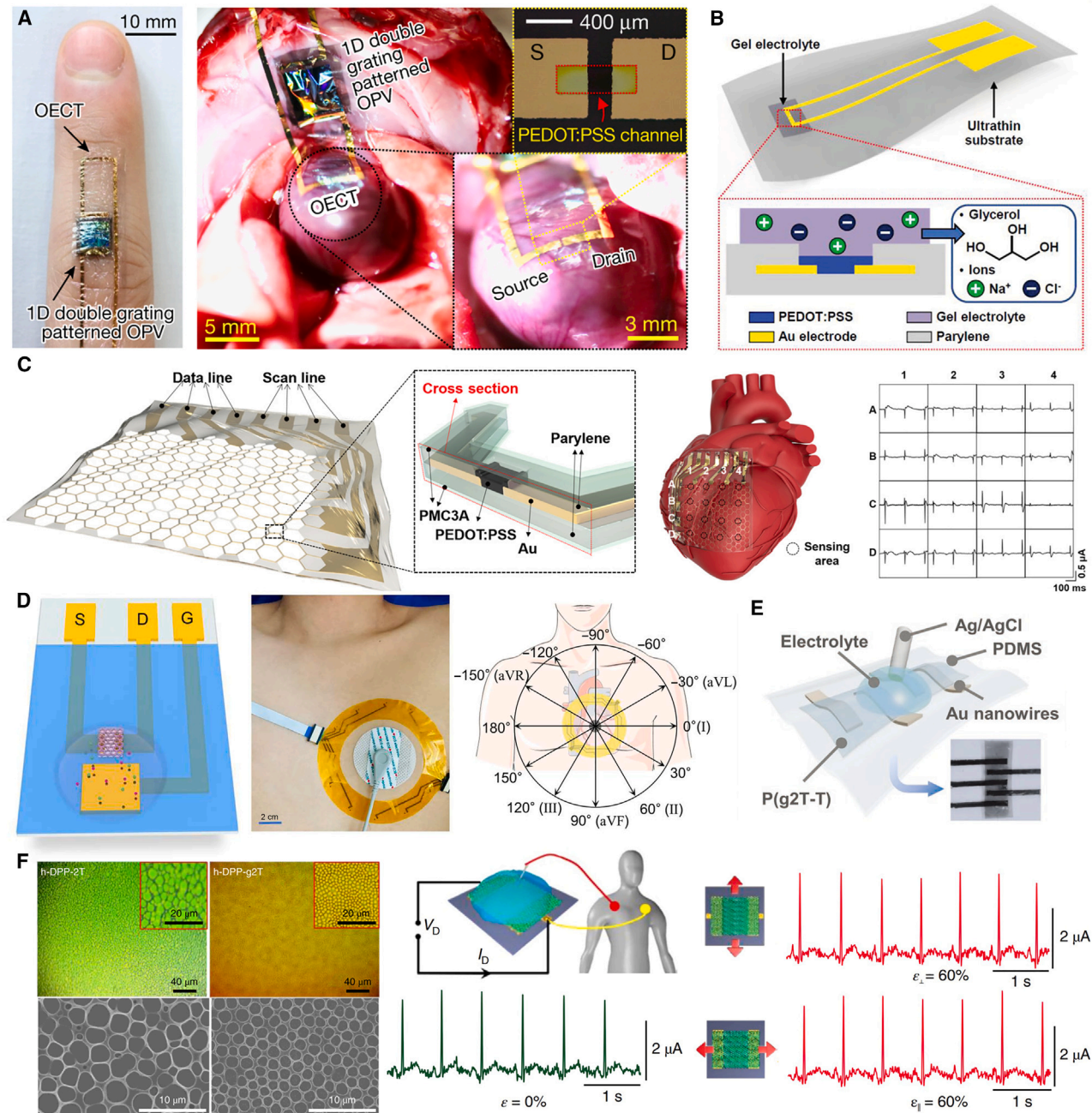


Figure 5. ECG monitoring using OECT-based biosensors

(A) Photograph of the OECT-integrated device attached to a finger and a rat heart. Reproduced with permission from Park et al.³² Copyright 2018, Springer Nature.

(B) Schematic diagram of an ultra-thin OECT with ion gel electrolyte. Reproduced with permission from Lee et al.³³ Copyright 2019, Wiley-VCH.

(C) Schematic of ultra-flexible OECTs based on honeycomb constructed arrays, developed for ECG monitoring. A 4 × 4 array was demonstrated by placing it on the heart of a rat. Reproduced with permission from Lee et al.³⁵ Copyright 2018, AAAS.

(D) Schematic of a Cu₃(HHTP)₂-based OECT attached to the human chest for monitoring ECG signals from different angles. Reproduced with permission from Song et al.³⁶ Copyright 2023, AAAS.

(E) Schematic diagram and photograph of stretchable OECTs attached onto a human wrist to measure ECG recordings. Reproduced with permission from Dai et al.¹⁸ Copyright 2022, Wiley-VCH.

(F) Optical and SEM images of the h-DPP-g2T layer, and OECTs using phs-h-DPP-g2T for measuring the ECG signals under different strains. Reproduced with permission from Chen et al.³⁷ Copyright 2022, Springer Nature.

poly(vinyl) alcohol (PVA) sacrificial layers onto glass substrates and transferred to biaxially pre-stretched styrene-ethylene-butylene-styrene (SEBS)/Cr/Au substrates after water immersion. The phs-h-DPP-g2T film demonstrated fold/collapse over 150% strains but retained the same morphology after the stretching and releasing process. OECTs using phs-h-DPP-g2T exhibited stable transfer characteristics, with only a slight degradation of maximum transconductance after 10,000 stretching cycles under 30% strains.

EMG signals are commonly utilized to evaluate the electrical activity of the skeletal muscles, providing essential insights into the underlying electrophysiological processes. To improve the accuracy and reliability of EMG signal measurements, Lee et al. have developed an ultra-flexible, high-temporal-resolution integrated device utilizing OECTs. By applying this device to a rat's gracilis muscle, typical muscle action potentials and accompanying contractions were detected with a fast response time of just 5 ms, as shown in [Figure 6A](#).¹¹⁰ To further enhance the fast response and sensitivity of physiologic sensing, an internal ion-gated structure was designed, utilizing a high-performance enhancement-mode OECT (e-IGT), which was made by de-doping PEODOT:PSS with polyethyleneimine ([Figure 6B](#)).³⁸ The e-IGT device exhibits rapid transient responses, with a response time of 2.9 μ s, and displays high spatiotemporal resolution, comparable to silicon-based amplifiers. Such ultra-flexible e-IGTs are capable of being conformably attached to human skin and have been employed to record both EMG and ECG signals.

EOG is a non-invasive technique utilized for measuring the electrical activity of the muscles surrounding the eye, providing valuable information for ophthalmological diagnosis and eye-movement tracking. Conventional EOG measurements have been performed using metal electrodes, which have limitations such as discomfort, low flexibility, and susceptibility to motion artifacts. To overcome these limitations, researchers have utilized flexible organic transistors for EOG recordings.³⁹ For instance, an ultra-flexible hybrid electrolyte-gated inverter was developed, comprising an n-channel indium gallium zinc oxide (IGZO)-based transistor and a p-type DPP-g2T-based OECT, for amplification and monitoring of EOG signals ([Figure 6C](#)). This device achieved 20-fold amplification, increasing the signal from around 1.5 mV to 30 mV, and realized an ultra-high gain of more than 110 under a low voltage of 0.7 V, demonstrating its potential for use in real-time EOG recordings with low power consumption and high gain.³⁹

Similarly, EEG recordings are one of the most frequently used techniques to study the function of neural networks in the brain, and are widely used in clinical settings for the diagnosis and monitoring of various neurological disorders such as epilepsy, sleep disorders, and brain injuries.¹¹¹ In a typical OECT-based EEG measurement, two OECTs were placed on the human scalp to record EEG signals and performed at good level on low-frequency recordings (1–8 Hz) due to the high transconductance of OECTs.¹¹² Recently, Spyropoulos et al. developed an OECT that enables integrated real-time sensing and stimulation during EEG recordings.⁴⁰ The OECT was based on internal ion-gated construction, and this unique design enables a self-(de-)doping process that eliminates the requirement for ion exchange with a shared external electrolyte. The ultra-small OECT can be effortlessly attached between hair follicles without the need for any chemical agents ([Figure 6D](#)), owing to the high amplification achieved through direct device-scalp interface. This results in a five-order-of-magnitude reduction in contact size, allowing for a more precise and accurate measurement of EEG signals.

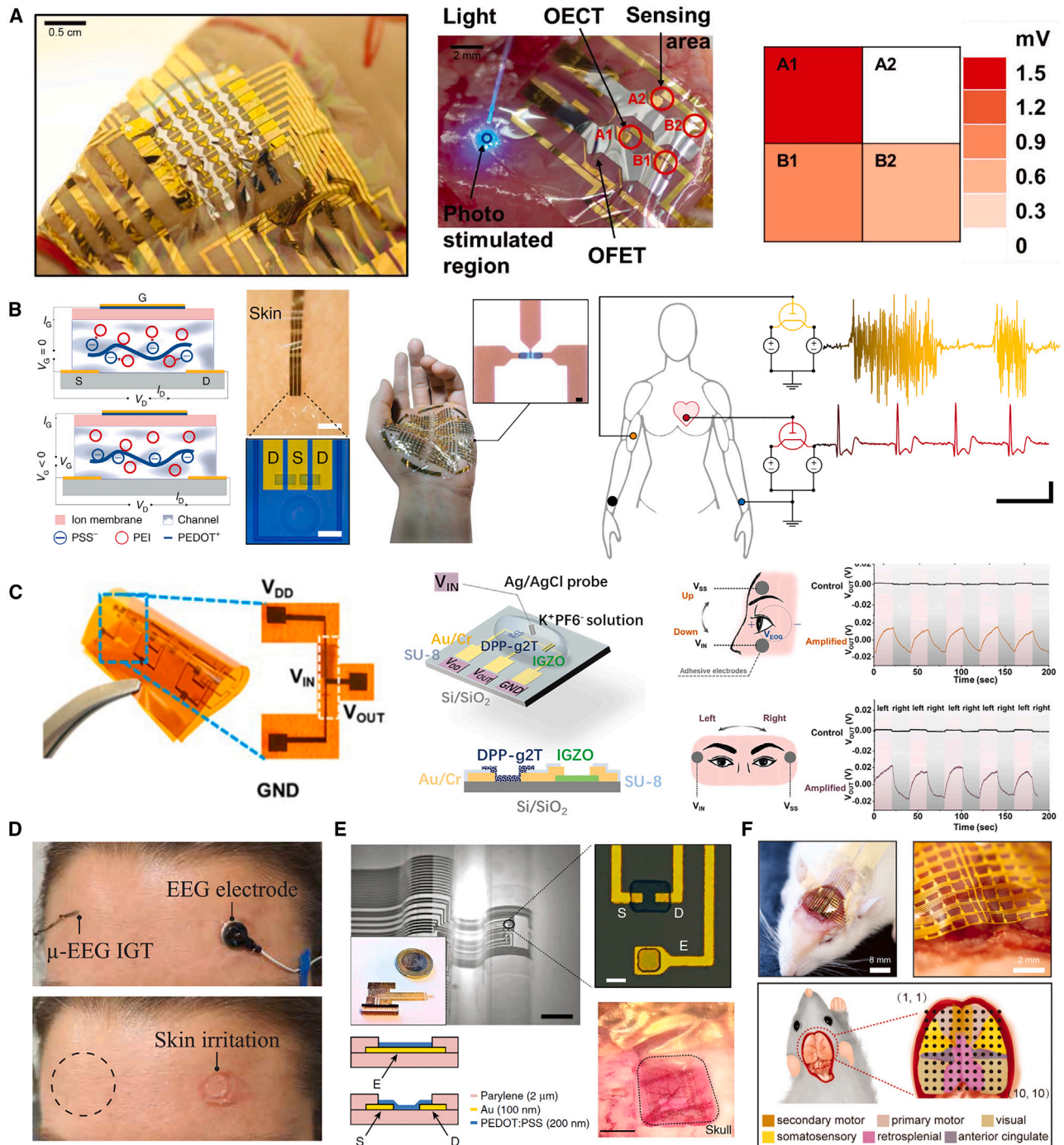


Figure 6. Various electrophysiological process detection using OEETs

(A) Photograph of an OEET-based multi-electrode array on a curved surface, attached to the surface of muscle tissue, and the corresponding spatial distribution of the EMG signal intensity. Reproduced with permission from Lee et al.¹¹⁰ Copyright 2016, Wiley-VCH.

(B) Structure of an e-IGT for ultra-flexible and conformable attachment to human skin, and its application for recording both EMG and ECG signals. Reproduced with permission from Cea et al.³⁸ Copyright 2020, Springer Nature.

(C) Schematic of an ultra-flexible hybrid electrolyte-gated inverter, composed of an n-channel IGZO-based transistor and a p-type DPP-g2T-based OEET, for amplification and monitoring of EOG signals. Reproduced with permission from Yao et al.³⁹ Copyright 2021, National Academy of Science.

(D) Photograph of an ultra-small OEET attached between hair follicles for EEG monitoring. Reproduced with permission from Spyropoulos et al.⁴⁰ Copyright 2019, AAAS.

Figure 6. Continued

(E) Optical images of a single OECT device and implantation of OECT arrays on the somatosensory cortex of rats to record ECoG signals. Reproduced with permission from Khodagholy et al.¹¹³ Copyright 2013, Springer Nature.

(F) Tissue-like OECT sensors with 100 channels, integrated into rats' cerebral cortex for cellular-level ECoG recordings. Reproduced with permission from Wu et al.⁴¹ Copyright 2023, Wiley-VCH.

ECoG is another technique used to measure the electrical activity of the brain. Unlike EEG, which involves placing electrodes on the scalp, ECoG requires the placement of electrodes directly on the surface of the brain. This approach provides a higher spatial resolution and more precise localization of the source of the electrical activity than EEG. Therefore, ECoG sensors must possess specific characteristics such as biocompatibility, high spatial resolution, stability, low noise, and flexibility to ensure accurate and reliable measurements. In 2013, Khodagholy et al. achieved a significant milestone in the development of ECoG sensors by firstly reporting the *in vivo* implementation of a biocompatible and flexible OECT for recording ECoG signals.¹¹³ They developed ultra-thin and flexible OECT arrays that could be conformed to the surface of the brain. These OECT arrays were subsequently implanted on the somatosensory cortex of rats to record ECoG signals (Figure 6E). Accurate identification of the regions of the brain that generate high-frequency oscillations or micro-seizures was successfully achieved. Mapping of brain activity caused by narcosis, epileptic seizure, and electric stimuli can be easily detected by integrating the tissue-like OECT sensors with 100 channels into rats' cerebral cortex (Figure 6F).⁴¹ This device displayed ultra-flexibility and biodegradability, with the 100 channels being able to receive the cellular-level ECoG recordings at the same time, which can be used as a neural interface. The development of these biosensors is crucial for advancing our understanding of brain function and treating neurological disorders.

Cell activity

In cell biosensing applications involving cells, it is crucial that the device and its bio-functionalization modifications are biocompatible and that the cell cultivation process is stable. In 2010, we developed OECT-based cell biosensors containing an eco-friendly and flexible poly(dimethylsiloxane) (PDMS) cell well on top of the active layers (Figure 7A),⁹⁶ where human esophageal squamous epithelial cancer cell lines (KYSE30) were cultivated on the PEDOT:PSS layer of the OECTs. The activities of the cancer cells were measured through an electrostatic interaction between the cells and the organic channel. To prevent membrane rupture and cell death caused by excessively high operation voltage across the tissue or cell layer, a solid-liquid dual-gate OECT was designed to measure the detachment of human mesenchymal stem cells, using poly(2,5-bis(3-triethyleneglycoloxythiophen-2-yl)-co-thiophene) (g2T-T) as the semiconducting channel material (Figure 7B).¹¹⁶ This design allowed for a voltage window of threshold voltage exceeding 0.3 V, broadening the material selection for cell-based organic bioelectronics.

To more accurately mimic organ and tissue systems *in vivo*, a tube-shaped OECT cell-sensing platform has been developed for 3D cell culture and real-time detection of its growth state (Figure 7C).⁴² The platform consists of porous PEDOT:PSS scaffold-based OECTs fixed in a T-shaped poly(vinylidene fluoride) (PVDF) tube, allowing for free flow of nutrients and mimicking the vasculature *in vivo*. Kidney epithelial cells and telomerase-immortalized fibroblasts were cultured in the device, and the transistor performance was compared, showing a significant difference in the drain current, efficiency of the ionic transduction, and relative change of response time between the two cell types, demonstrating the potential for screening multiple cell types.

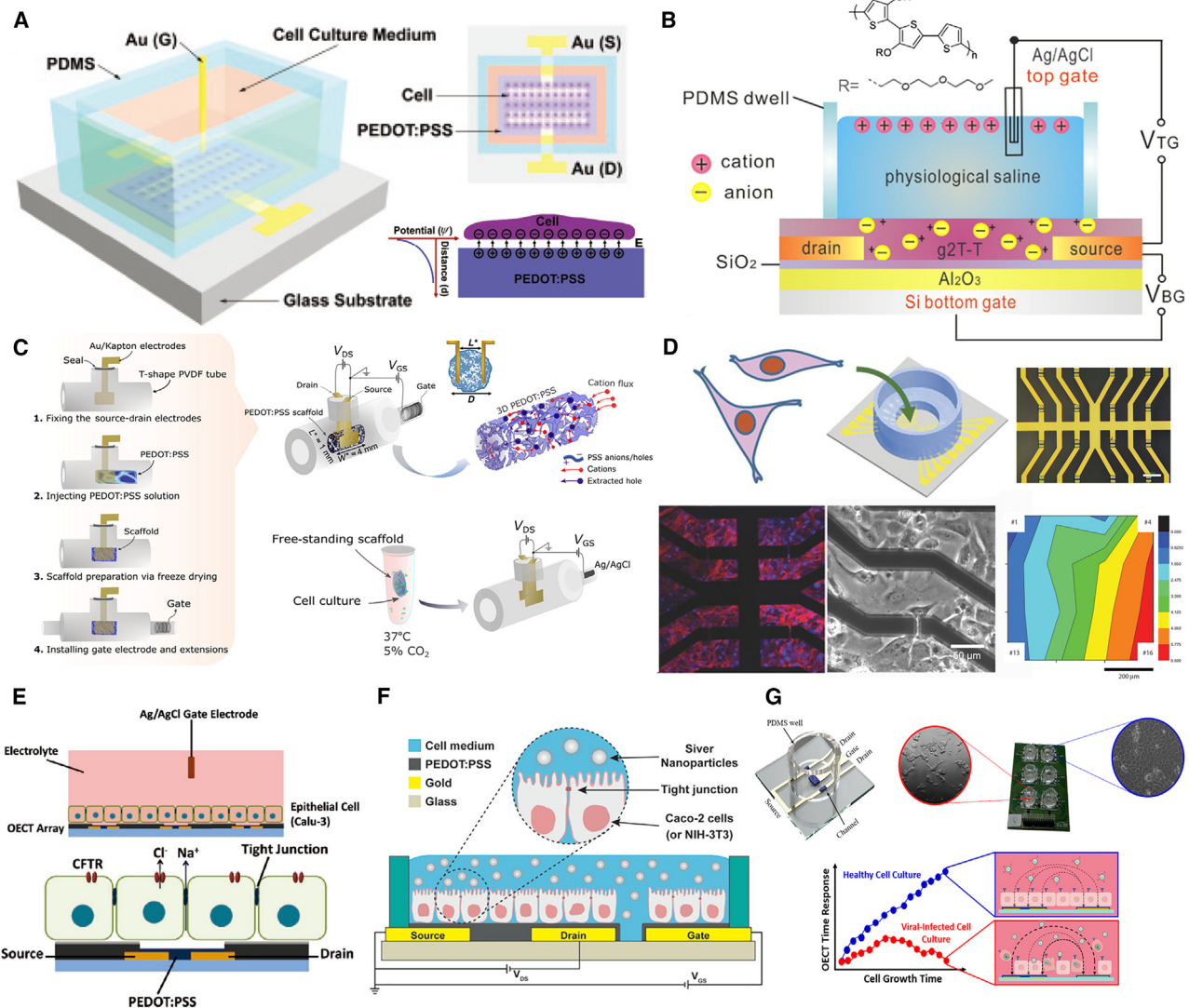


Figure 7. Demonstration of cell-based OECT biosensors

(A) Schematic of human esophageal squamous epithelial cancer cell lines cultured on the surface of OECTs. Reproduced with permission from Lin et al.⁹⁶ Copyright 2010, Wiley-VCH.

(B) Schematic diagram of the cross-sectional structure of g2T-T based OECTs. Reproduced with permission from Zhang et al.¹¹⁶ Copyright 2017, American Chemical Society.

(C) Fabrication process of a tube-shaped OECT cell-sensing platform. Reproduced with permission from Pitsalidis et al.⁴² Copyright 2018, AAAS.

(D) Schematic diagram of 16-channel OECT array and distribution map of action potentials in primary cardiomyocytes. Reproduced with permission from Gu et al.¹¹⁷ Copyright 2017, Wiley-VCH.

(E) Schematic diagram of human airway epithelial Calu-3 cells cultured on an OECT array. Reproduced with permission from Yao et al.⁹⁵ Copyright 2013, Wiley-VCH.

(F) Cross-sectional schematic of a cell-based OECT, with Caco-2 cell layers seeded on OECT channels. Reproduced with permission from Decataldo et al.⁴⁶ Copyright 2020, Wiley-VCH.

(G) Healthy and virus-infected cells were cultured in the channel areas of PEDOT:PSS-based OECTs and enclosed in a perforated cylinder made of PDMS, respectively. Reproduced with permission from Decataldo et al.⁴⁴ Copyright 2022, Springer Nature.

As cell culture is a complicated process, effective strategies should be adopted for high biocompatibility, low cell infection, and slow device degradation. A novel 16-channel OECT-based cell biosensor was developed to study the physiological activities of a rat cardiomyocyte monolayer during long-term culturing (Figure 7D).¹¹⁷ Ten synchronous action potentials could be recorded to quantitatively characterize

the electrophysiological behavior of cardiomyocytes. The devices were modified with fibronectin before cell seeding to improve their biocompatibility. Another example involved depositing extracellular matrix-derived polypeptide poly(L-lysine) (PLL) on a PEDOT:PSS film before adding PVA solution into the film to enhance its covalent linkage abilities with biological moieties.¹¹⁸ Perfect growth and differentiated status of neuron cell line PC12 on PLL-functionalized PEDOT:PSS:PVA patterns show great potential for application in OECT-based cell biosensors.

High time resolution is an available strategy for cell biosensing, whereby an OECT array is integrated with human airway epithelial Calu-3 cells (Figure 7E).⁹⁵ This integration provides a novel method to couple transepithelial ion transport with electric current, and activation as well as inhibition of transepithelial ion transport can be readily detected with excellent time resolution. Furthermore, to achieve fast and real-time cell monitoring, PEDOT:PSS-based OECTs with both vertical and planar configuration have been fabricated.⁴³ The leaky-barrier model cells (NIH-3T3, mouse fibroblasts) and strong-barrier cells (Caco-2, human colorectal epithelia) were seeded directly on the channel areas, and tissue growth and detachment could be continuously monitored through transistor dynamic behavior for monitoring of the cellular vitality.

Cell-based OECTs have significant implications in various areas, including disease diagnosis,⁴⁴ drug delivery,⁴⁵ nanomaterial toxicity evaluation,⁴⁶ cell-surface glycans,⁵¹ and single-cell detection.^{49,50} One specific application of OECTs is for the assessment of nanomaterial safety. Toxic citrate-coated Ag NPs have been found to strongly affect ion fluxes through Caco-2 cell layers seeded on OECT channels (Figure 7F), while non-toxic citrate molecules do not have this ability.⁴⁶ This demonstrates that OECTs can provide a non-invasive and label-free method for real-time monitoring of nanomaterial toxicity. Moreover, a similar design of OECTs has been used to detect the cytopathic effect of inducing severe acute respiratory syndrome (SARS) virus on Vero E6 cell lines.⁴⁴ In this case, healthy and virus-infected cells were cultured in the channel areas of PEDOT:PSS-based OECTs and enclosed in a PDMS perforated cylinder, respectively (Figure 7G). This technology has the potential to be adapted for assessing the neutralizing antibody response toward different viruses in various species, allowing for investigation of their role in the ecology of infection. In addition, cell-based OECTs have been used to detect the growth of bacteria, such as *Salmonella*⁵³ and *Pseudomonas fluorescens*.⁵²

BIOINFORMATICS ANALYSIS

Bioinformatics involves the analysis of various biological molecules and processes in human body fluids such as blood, serum, sweat, saliva, tears, and urine. These fluids contain important biomarkers such as ion concentrations, metabolites, hormones, neurotransmitters, nucleic acids, and proteins. OECTs have been shown to have good sensing performance in aqueous solutions, making them a promising tool for acquiring bioinformation from human body fluids. OECTs can be functionalized with specific receptors or enzymes to selectively detect and quantify analytes of interest, such as glucose, lactate, dopamine, DNA, RNA, antigen, or antibody. With their high sensitivity, low cost, and compatibility with flexible and wearable devices, OECT-based biosensors have the potential to revolutionize the field of healthcare by enabling continuous non-invasive monitoring of biomarkers in real time. The objective of this section is to present an in-depth review of the latest developments in OECT-based biosensors for bioinformatics analysis from human body fluids. To illustrate the significant findings in this field we refer the reader to Table 2, which provides a summary of the most important discoveries.

Ions and pH

Ion sensing is a crucial aspect in numerous fields, including environmental monitoring, medical diagnosis, and industrial manufacturing. Biologically important ions such as K^+ , Na^+ , Ca^{2+} , and Cl^- are widely utilized for disease diagnosis globally.¹¹⁹ OECT-based ion biosensors have been extensively developed owing to the high sensitivity of OMIECs to ion doping, particularly in bodily fluids such as tears, sweat, saliva, and urine.^{54–57} Recently, a self-powered OECT-based contact lens has been reported that can detect Ca^{2+} levels in tears and has demonstrated excellent ion selectivity (Figure 8A). Elevated Ca^{2+} levels have been linked to impaired glucose metabolism, indicating that OECTs for ocular monitoring have potential to evaluate the risk of diabetes.⁵⁴

Sweat analysis is another area where ion sensing is widely applied, and a typical sweat ion OECT-based biosensor has been developed using a PEDOT:PSS/[MTEOA][MeOSO₃] channel material and a lipophilic salt sodium tetrakis[3,5-bis(trifluoromethyl)phenyl] borate (Na-TFPB) ISM (Figure 8B).⁵⁶ The device shows real-time changes in drain current in response to Na^+ and K^+ under fast response time of around 40.57 μs (Figure 8C). To achieve continuous sweat ion monitoring, a flexible, skin-mountable, fiber-based OECT has been developed using a simple wet-spinning process (Figure 8D).⁵⁵ The channel layer is composed of PEDOT:PSS microfibers that are produced by wet-spinning in aqueous sulfuric acid solutions, and these microfibers are then attached to Ag wires using silver epoxy coating for source and drain contacts. To form a source-gate hybrid electrode, the unpassivated silver epoxy is chlorinated using clorox solution, resulting in the formation of Ag/AgCl. This two-terminal single-strand fiber-based OECT can be comfortably worn on the arm or integrated into garments for the direct and continuous detection of cations in real time.

The nitrate ion can serve as a potential biomarker for mental stress in biofluids, as it can indicate the activity of the autonomic nervous system and its response to stress.⁵⁸ Recently, Takemoto et al. have developed a fully transparent OECT with a nitrate-ion-selective gate electrode for the detection of nitrate ions (Figure 8E). The device has demonstrated a linear detection range of 10 μM to 10 mM, which is appropriate for monitoring salivary nitrate levels.⁵⁸ This technology has potential applications in the non-invasive monitoring of mental stress through the analysis of nitrate levels in saliva.

pH sensing involves the detection of hydrogen ion (H^+) and bicarbonate ion (HCO_3^-) concentration, which are important indicators of acidity or alkalinity. Similar to ion sensing, hydrogen ISMs are commonly used in the fabrication of pH-based OECTs. However, these OECT-based pH sensors with ISM typically use aqueous electrolytes as the dielectric layer, which can lead to fouling or device degradation due to the leakage or evaporation of human sweat.^{120,121} To address this issue, Chen et al. have developed an ion-gel layer as a solid electrolyte for pH monitoring.⁵⁷ This ion-gel layer was synthesized using pH-sensitive bromothymol blue blended with the intrinsic hydrophobicity of 1-butyl-3-methylimidazolium bis(trifluoromethylsulfonfyl)imide ([BMIM][TFSI]) and the copolymer poly(vinylidene fluoride co-hexafluoropropylene) (PVDF-HFP) (Figure 8F). The OECTs with the ion-gel layer demonstrated a pH sensitivity of up to 91 mA dec⁻¹ when detecting pH values ranging from 2 to 7. In addition, the devices exhibited good mechanical flexibility, with no significant current degradation observed even when the OECT was bent at curvatures with bending radii of 30 mm. Furthermore, the devices showed only a 20% decrease in transconductance after 500 bending cycles.

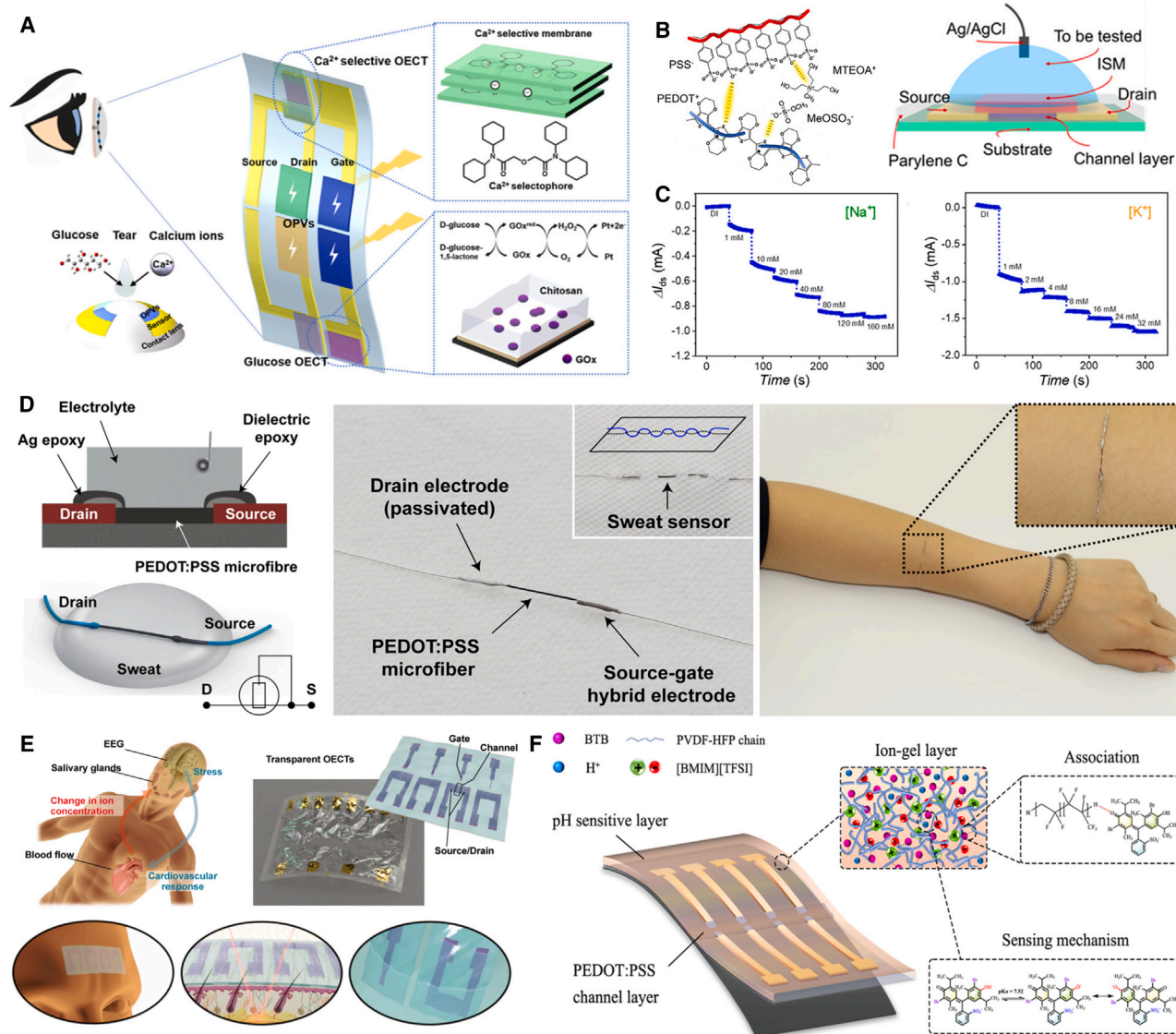


Figure 8. Applications of OECTs in ion sensing

(A) Schematic of a self-powered OECT-based contact lens for detection Ca^{2+} levels in tears. Reproduced with permission from Lin et al.⁵⁴ Copyright 2022, Springer Nature.

(B) Chemical structures of the PEDOT:PSS/[MTEOA][MeOSO₃] channel material and schematic of an OECT with ion-selective membrane.

(C) The real-time changes in source/drain current in response to variations in Na^{+} and K^{+} concentrations. (B) and (C) reproduced with permission from Li et al.⁵⁶ Copyright 2022, American Chemical Society.

(D) Schematic of a fiber-based OECT composed of PEDOT:PSS microfibers, which can be comfortably worn on the arm. Reproduced with permission from Kim et al.⁵⁵ Copyright 2018, Springer Nature.

(E) Schematic of a fully transparent OECT for various bioelectronic applications. Reproduced with permission from Takemoto et al.⁵⁸ Copyright 2023, Wiley-VCH.

(F) Schematic of pH-sensitive OECTs, which consist of a pH-sensitive layer, an ion-gel layer, and a PEDOT:PSS channel layer. Reproduced with permission from Chen et al.⁵⁷ Copyright 2023, Royal Society of Chemistry.

Biological small molecule

Biological small molecules are fundamental components of larger biological molecules, including lipids, phospholipids, amino acids, steroids, glycolipids, vitamins, hormones, neurotransmitters, carbohydrates, and sugars. These molecules play crucial roles in various biological processes and are essential for human life.

Metabolites are a subset of biological small molecules that are produced or consumed through metabolic processes. Analysis of specific metabolites, such as glucose, lactate, and cholesterol, is a crucially important approach for early diagnosis of related diseases. For example, glucose monitoring is the gold standard for diagnosis and prevention of diabetes mellitus, and OECT-based glucose sensors came into being based on the reaction of glucose and GOx. Liao et al. used functional gate electrode with modification of a polyaniline (PANI)/Nafion-graphene bilayer to improve the selectivity of the OECT-based biosensor, in which PANI and Nafion film can repel the positively and negatively charged molecules, respectively (Figure 9A).¹⁰⁰ The glucose in human saliva was further measured with this OECT, achieving non-invasive glucose monitoring. With a similar sensing mechanism, replacing GOx with urate oxidase (UOx) enabled the realization of an OECT-based uric acid biosensor. Furthermore, a self-powered OECT-based glucose biosensor has been developed by using NDI-T2 copolymer serving as electron-transporting material. By drawing the energy from glucose present naturally in all bodily fluids, the prepared reversible, mediator-free, miniaturized OECT sensors achieved excellent stability for in excess of 30 days (Figure 9B).⁵⁹ Moreover, the quantification of metabolites in the human brain, particularly ascorbic acid, which serves as an essential antioxidant and neuromodulator in the central nervous system, has been successfully achieved using soft-fiber-based OECTs.^{122,123}

Lactate production is known to be associated with glucose uptake and usage, making lactate an essential metabolite for health monitoring.¹²⁴ To detect lactate, functionalized OECTs were fabricated and integrated into a lactate detection platform. The lactate in tumor cells reacts with enzymes on the gate electrodes of OECTs, altering electrochemical sensing signals.¹²⁵ However, efficient use of enzymes in biosensing is crucial and requires effective electrical communication between the redox centers of the protein and the transducing electrode. To address this issue, LOx was immobilized directly on top of a copolymer P-90 semiconducting layer through glycol side chains that provide polar groups to interact with the enzyme (Figure 9C). The resulting OECTs exhibited a wide dynamic range of lactate detection, from 10 μ M to 10 mM, and a rapid response time of within 2 s.⁶⁵ Additionally, the elimination of mediators and the external reference electrode simplifies the device type's adoption into various structures and functions.

Given the ultra-sensitivity of OECTs in aqueous solutions, there has been growing interest in exploring non-invasive metabolic or hormonal detection in body fluids such as saliva, sweat, tears, interstitial fluid, and others.^{100,71,102,105,63,72} One example of this is the selective detection of sweat cortisol using OECTs with a biomimetic polymeric membrane-based detecting platform. This platform consists of laser-patterned microcapillary channel arrays, a sample reservoir, a molecularly selective OECT, and a waterproof protection layer, as shown in Figure 9D.⁷¹ Notably, the OECTs fabricated on a SEBS elastomer substrate exhibit excellent flexibility and stretchability, enabling an optimal fit when attached to human skin. The biomimetic polymeric membrane serves as a molecular memory layer, facilitating controllable and regulated transport of cortisol molecules. Owing to the complex composition of body fluids, multi-analyte OECT-based microarrays with finger-powered pumping were developed for quantitative screening of glucose, lactate, and cholesterol levels as shown in Figure 9E.¹⁰² Under a pumping actuation force with a human finger, biological samples such as blood or saliva can be driven inside the microchannel, achieving multiplexed, non-invasive, and personalized point-of-care diagnostics.

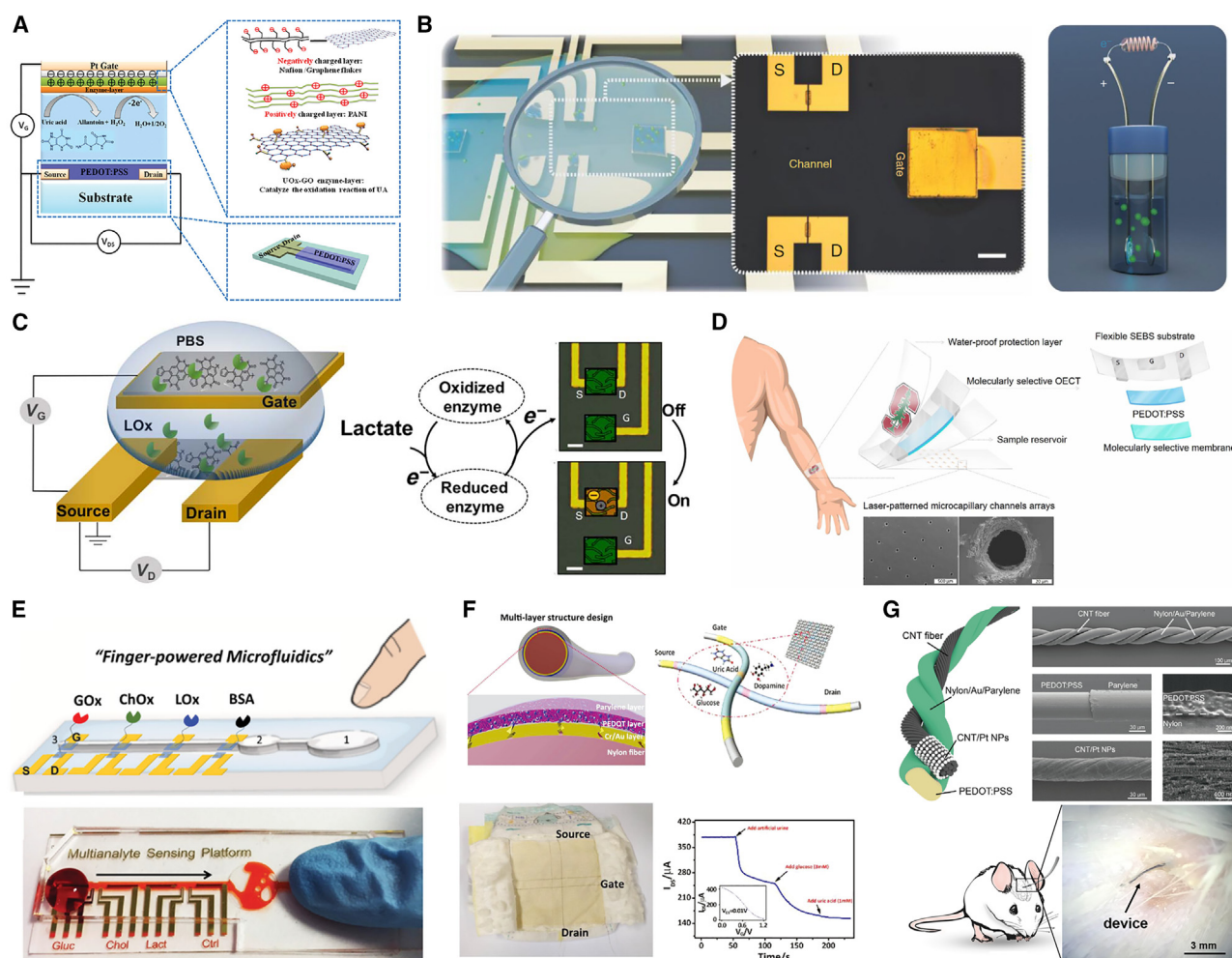


Figure 9. Biomolecule detection using OECTs, including metabolites, hormones, and neurotransmitters

(A) Schematic diagrams of OECTs modified with PANI/Nafion-graphene bilayer. Reproduced with permission from Liao et al.¹⁰⁰ Copyright 2015, Wiley-VCH.

(B) Illustration of the OECT-based glucose biosensor. Reproduced with permission from Ohayon et al.⁵⁹ Copyright 2020, Springer Nature.

(C) Schematic of lactate-sensitive OECTs and the interaction between lactate oxidase (LOx) and lactate, which occurs on top of a copolymer P-90 semiconducting layer. Reproduced with permission from Pappa et al.⁶⁵ Copyright 2018, AAAS.

(D) Schematic of OECTs with a biomimetic polymeric membrane-based detecting platform and SEM images of laser-patterned microcapillary channels arrays. Reproduced with permission from Parlak et al.⁷¹ Copyright 2018, AAAS.

(E) Schematic diagram and photograph of OECT array with finger-powered microfluidics. Reproduced with permission from Pappa et al.¹⁰² Copyright 2016, Wiley-VCH.

(F) Schematic diagrams of a fabric OECT biosensor, photograph of integration of OECT into a diaper, and a sensing response with additions of artificial urine containing different concentrations of glucose. Reproduced with permission from Yang et al.⁶¹ Copyright 2018, Wiley-VCH.

(G) Schematic diagrams and SEM images of fiber-based OECTs with platinum nanoparticles-modified CNT fiber gate electrodes, and photograph of fiber-based OECTs implanted in mouse brain. Reproduced with permission from Wu et al.⁶² Copyright 2020, Springer Nature.

To further expand the application of OECTs in wearable electronics, a typical glucose biosensor was microfabricated on nylon fiber with a multilayer structure composed of high-conductive metal/polymer double-layer electrodes, a PEDOT:PSS semiconductor channel, and a parylene isolation layer (Figure 9F).⁶¹ The PEDOT:PSS layer can connect the cracks in metal during the bending process, resulting in the Cr/Au/PEDOT electrodes exhibiting a stable conductivity to minimize the voltage drop after 5,000 bending tests. The fabric-based OECTs can be integrated in a diaper and remotely controlled with a smartphone, showing a clear

response with additions of artificial urine containing different concentrations of glucose. The precise and continuous health monitoring of fiber-based OECTs helps to personalize healthcare and diagnose early. Following the concept of fiber-based OECTs, Wu et al. developed carbon nanotube (CNT) fiber-based OECT multi-analyte biosensors for detection of metabolites, neurotransmitters, and amino acids, including glucose, dopamine, and glutamate, in deep tissues that are typically difficult to access.⁶² Modification of CNT fiber gate electrodes with platinum nanoparticles improves the low detection limit and high sensitivity of OECTs. The arbitrary deformation properties that thin-film transistors do not possess allow fiber-based OECTs to maintain dimensional stabilities in physiological environments after implantation in mouse brain (Figure 9G). This achievement enables 7-day continuous neurotransmitter dopamine monitoring *in vivo* with excellent biocompatibility. Benefiting from the interaction between the channel area and the electrolyte near the fiber surface, fiber-based OECTs are insensitive to geometric deformation, thus providing more possibilities for application scenarios.

Nucleic acid

Nucleic acid analysis, involving both DNA and RNA, has emerged as a pivotal technique in many biological processes and has garnered significant attention in diagnostic and therapeutic applications. It finds applications in gene expression profiling, detection of biowarfare and bioterrorism agents, identification of viral and bacterial pathogens, and clinical medicine, among others.^{97,126} OECTs have recently been applied to nucleic acid detection, offering a portable, accurate, and convenient alternative to gold-standard methods such as PCR.

One common method for creating OECT-based DNA sensors involves immobilizing DNA molecules onto the OMIECs layer or electrodes. This process typically involves hybridizing single-stranded DNA (ssDNA) with its complementary DNA to form double-stranded DNA. Our group developed a typical OECT-based DNA biosensor with an integrated microfluidic channel on a polyethylene terephthalate (PET) substrate in 2011.⁹⁷ The ssDNA was immobilized on the Au gate surface through covalent bonding, and the complementary DNA was introduced into the microfluidic channel where it hybridized with the ssDNA (Figure 10A). This device could detect DNA targets at concentrations as low as 1 nM, and the detection limit was extended to 10 pM by applying an electric pulse. However, most methods of fixing DNA by gold-thiol bonds require encapsulation to minimize the non-specific adsorption of interference biomolecules.¹²⁷ To simplify this step, Sensi et al. proposed using poly-dopamine (PDA), which can be spontaneously polymerized on the carbon gate electrodes of OECTs and facilitate immobilization through Michael additions or Schiff base reactions between PDA and active groups at the 5' or 3' end of ssDNA. This resulted in a more effective detection method for complementary DNA strands, with an LOD of 100 fM and a linear range over four orders of magnitude.⁷⁸

Song et al. developed a photosensitive OECT by integrating a photoelectrochemical active gate electrode, resulting in a higher-sensitivity DNA biosensor. The ssDNA was immobilized on CdS quantum dots (QDs) and could capture the target DNA labeled with Au NPs (Figure 10B). The interaction between excitons and plasmons between CdS QDs and Au NPs influenced the charge transfer on the gate electrode.⁷⁷ The device was capable of detecting the concentration of target DNA down to 1 fM due to its amplification function. Organic photoelectrochemical transistors (OPECTs) have also been used to detect microRNA (miRNA).^{128,79} TiO₂ nanotubes incorporated with CdS QDs were modified on the gate of OPECTs to perform hybridization chain reaction amplification, with the aim of detecting the biomarker

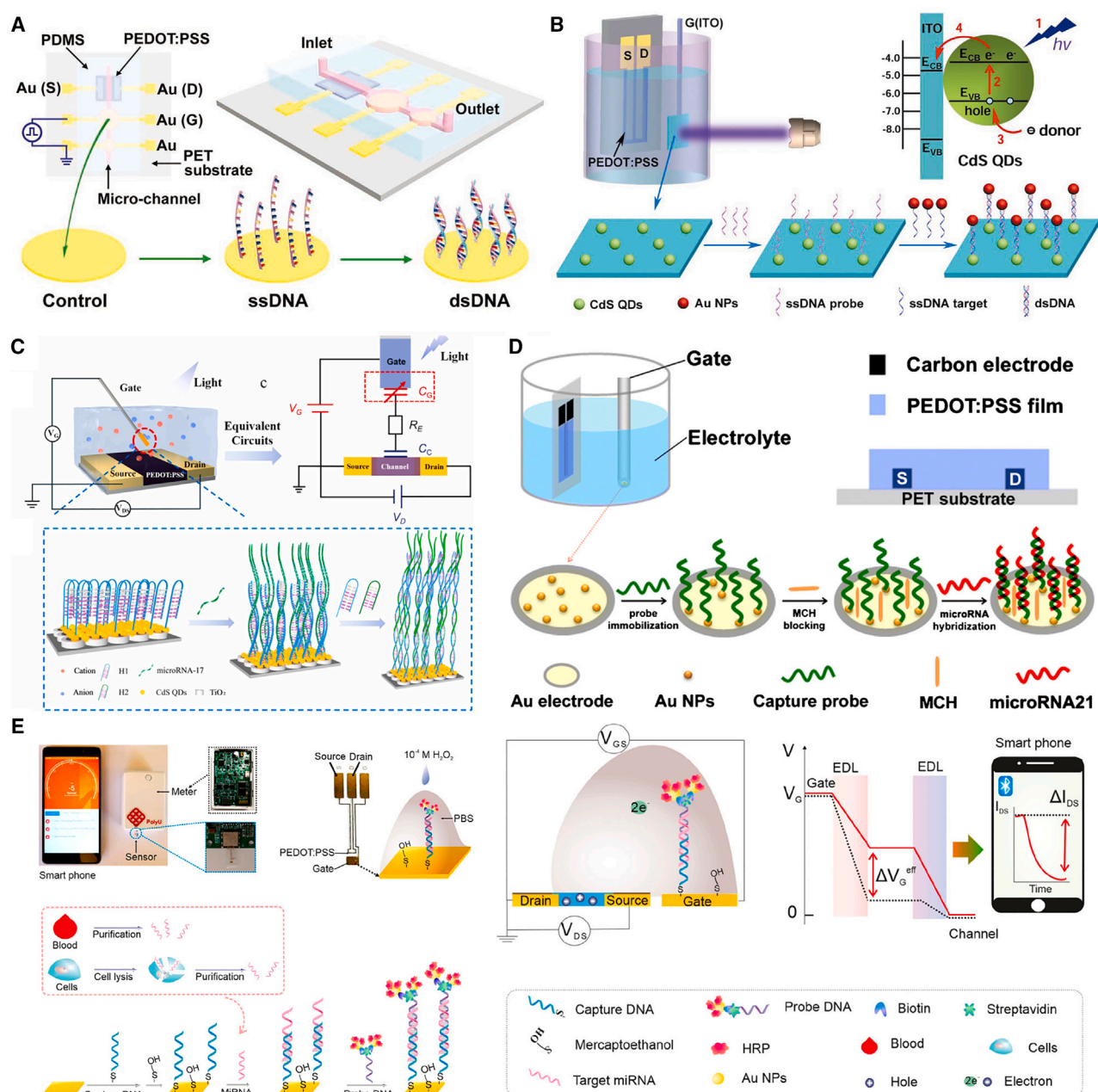


Figure 10. Fabrication process of nucleic acid-based OECTs

(A) Schematic diagram of an OECT-based DNA biosensor with an integrated microfluidic channel on a PET substrate, and hybridization process between ssDNA and target DNA on the Au gate. Reproduced with permission from Lin et al.⁷⁷ Copyright 2011, Wiley-VCH.

(B) Schematic of a photosensitive OECT, in which the gate electrode consists of CdS QDs, Au NPs, and ssDNA, for capturing the target DNA. Reproduced with permission from Song et al.⁷⁷ Copyright 2018, Wiley-VCH.

(C) Schematic of an OECT with gate modification of TiO₂ nanotubes and CdS QDs for detecting the miRNA-17. Reproduced with permission from Gao et al.⁷⁹ Copyright 2022, Elsevier.

(D) Gate-modification process of RNA-based OECTs. MCH, mercapto-1-hexanol. Reproduced with permission from Peng et al.⁸⁰ Copyright 2018, Springer Nature.

(E) Schematic diagrams of an OECT-based RNA sensing platform for detecting miRNA21 from breast cancer cells controlled by a smartphone. Reproduced with permission from Fu et al.⁸¹ Copyright 2021, American Chemical Society.

miRNA-17 as the target analyte (Figure 10C). The inherent amplification function and photoelectrochemical analysis advantages of OECTs enable the detection of miRNA-17 with ultra-low concentrations down to 1 pM.⁷⁹ Additionally, OECTs are widely used in other biological sensing and pathological examinations, including enzyme-associated analysis,^{129,130} body fluid biomarker monitoring,⁸⁴ and antibody/antigen detection.^{85,131}

RNA is more susceptible to degradation compared to DNA, due to its single-stranded structure and the presence of ribonucleases (RNases) that can cleave RNA molecules. To address this issue, a gold electrode was modified with Au NPs to immobilize the DNA probe for capturing miRNA21 extracted from HeLa cells.⁸⁰ Prior to the hybridization process, 6-mercapto-1-hexanol was used to block the degradation effect of miRNA21 (Figure 10D). The resulting OECTs demonstrated high sensitivity and specificity, enabling the detection of miRNA21, which is highly expressed in many types of cancers. This approach has the potential for early diagnosis of various diseases, including cancer, cardiovascular disease, diabetes, and neurodegenerative disorders. Recently, our team has developed a highly sensitive biosensing platform based on OECTs for detecting miRNA21 from breast cancer cells.⁸¹ This platform consists of a disposable OECT, a portable meter, and a smartphone, which work together to enable the detection of miRNA21 cancer biomarkers from low-volume solutions with concentrations as low as 10^{-14} M (Figure 10E). The OECT's wide detection range over nine orders of magnitude, from 10^{-14} to 10^{-6} M, is remarkable and enables the distinction of miRNA expression levels in blood samples at different stages of cancer. This capability holds great potential for early diagnosis and improved treatment outcomes for cancer patients.

Protein

The recognition of antibodies and antigens is a critical step in the early detection of pathological conditions and the development of targeted therapies. Various techniques such as enzyme-linked immunosorbent assays, optical measurements, and electrochemical biosensing have been employed for this specific binding reaction. However, most of these methods are time-consuming and require lengthy experimental procedures, in addition to relying on expensive instruments and professional operation methods, which can complicate early diagnosis in patients. Fortunately, OECT-based protein biosensors have recently emerged as a promising diagnostic platform.^{83,86,87} These biosensors offer several advantages, such as high sensitivity and selectivity, low cost, rapid detection, point-of-care capabilities, easy operation, and personalized applications, when compared to traditional immunoassay methods. Researchers have demonstrated that modifying the gate electrode or organic channel layer significantly improves the sensing performance of OECT-based protein biosensors.^{99,88–90}

An OECT-based protein biosensor that can chirally recognize α -amino acid has been achieved with modified molecularly imprinted polymer films on the gate electrodes. L-Tryptophan (L-Trp) molecules can occupy the complementary cavities in the polymer matrix through non-covalent interactions, as shown in Figure 11A.⁸⁹ Additionally, Fu et al. fabricated an ultra-high-sensitive OECT for detecting a cancer biomarker, human epidermal growth factor receptor 2 (HER2) (Figure 11B),⁹⁹ in which Au NPs, HER2 detection antibody, and enzyme horseradish peroxidase (HRP) together worked as nanoprobe on the electrode surface to achieve detection down to the concentration of 10^{-14} g mL⁻¹.

OECTs can be rendered selectively by incorporating biorecognition components, such as a microfluidic-channel-based OECT with a nanoporous membrane

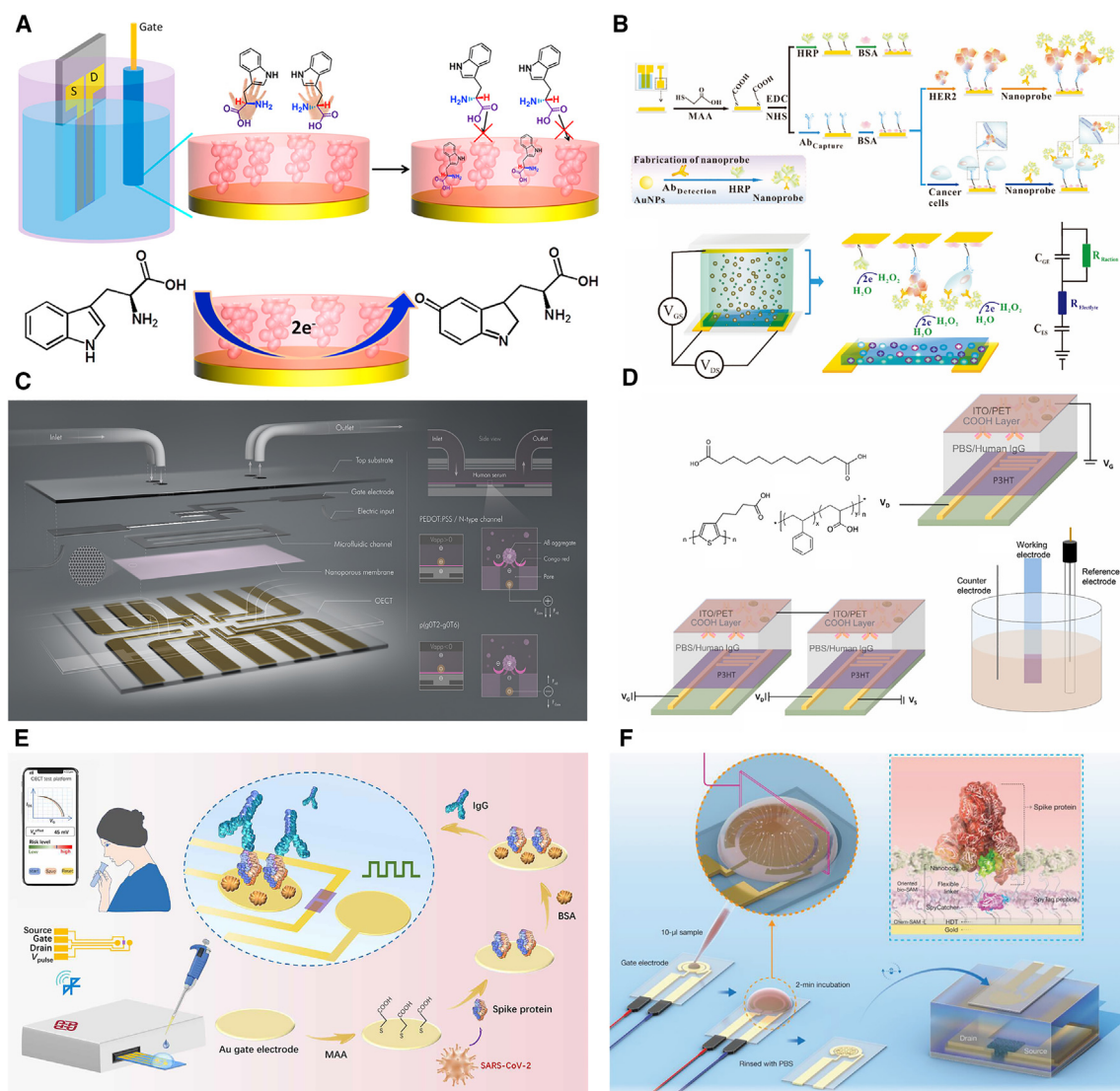


Figure 11. Typical application of protein-based OECTs for different disease diagnosis

(A) Schematic of an L-Trp-based OECT for recognizing α -amino acid. Reproduced with permission from Zhang et al.⁸⁹ Copyright 2018, Elsevier.

(B) Fabrication process of ultra-high-sensitivity OECTs for detecting a cancer biomarker. Reproduced with permission from Fu et al.⁹⁹ Copyright 2017, Wiley-VCH.

(C) Schematic of a microfluidic channel-based OECT with a nanoporous membrane functionalized with Congo red molecules. Reproduced with permission from Koklu et al.⁹⁰ Copyright 2021, American Chemical Society.

(D) Schematic of anti-IgG antibodies functionalized D-OECTs. Reproduced with permission from Song et al.⁹¹ Copyright 2022, Elsevier.

(E) OECT-based antibody detection platform for SARS-CoV-2 IgG detection. Reproduced with permission from Liu et al.⁸³ Copyright 2021, AAAS.

(F) Schematic diagrams and operation processes of enhanced nanobody-functionalized OECTs. Reproduced with permission from Koklu et al.⁸⁷ Copyright 2022, Wiley-VCH.

functionalized with Congo red molecules (Figure 11C). This biosensor has demonstrated a strong affinity for amyloid- β ($A\beta$) aggregates, allowing for high discrimination of hybrid $A\beta$ charges at various concentrations.⁹⁰ The aggregation of $A\beta$ in the human brain is a precursor to Alzheimer's disease, making the detection of $A\beta$ aggregates an important diagnostic tool. Moreover, dual-gate configurations of OECTs (D-OECTs) can improve the accuracy of protein detection.⁹¹ In the case of detecting immunoglobulin G (IgG), the two same gate electrodes of D-OECTs are functionalized with anti-IgG antibodies and other polymers in the same way

(Figure 11D). This approach leads to a significant reduction or even elimination of voltage drifts, as the drifts occur in opposite polarities with respect to the direction of the gate voltage probe on the two gates as compared to single-gate designs. The detection limit of D-OECTs for IgG was found to be 0.07 aM, indicating that D-OECTs could be an attractive option for a variety of clinical diagnostic applications requiring the detection of low concentrations of IgG.

Recently, OECT-based protein biosensors have been used for detecting antibodies or antigens of the acute respiratory syndrome coronavirus 2 (SARS-CoV-2) that has caused the global spread of coronavirus disease 2019 (COVID-19) since January 2020. To address this pressing need, we have developed an OECT-based antibody detection platform, as depicted in Figure 11E.⁸³ The SARS-CoV-2 spike protein was captured via conjugation between amine groups and carboxylic groups on the surface of Au gate electrodes. To ensure specific detection, any remaining non-specific binding sites of the gate electrode were coated with BSA. After optimizing the Debye length, pH values, and operation voltage pulses, this platform can detect SARS-CoV-2 IgG within 5 min, and the detection limit of 10 fM is sufficient to meet the detection range in human serum and saliva. Conversely, to detect the SARS-CoV-2 spike protein, a single-chain antibody was immobilized on the sensing layer of OECTs. In particular, Koklu et al. employed a single-chain antibody linked to a SpyCatcher domain via a flexible linker (Figure 11F).⁸⁷ This enabled the antibody to be fixed to the OECT surface in a controlled molecular orientation and configuration. Additionally, they developed nanobody-functionalized OECTs for detecting the spike protein of coronavirus, which can detect even a single molecule corresponding to a concentration of 0.33 aM.⁸² This state-of-the-art biosensor platform holds great promise for rapid, ultra-sensitive, and specific detection of both SARS-CoV-2 and Middle East respiratory syndrome coronavirus (MERS-CoV) antigens.

BIOMIMETIC DEVICES

Biomimetic devices are engineered to replicate the structure or function of biological systems found in nature using the principles of biomimicry. These devices encompass a wide range, from simple structures that imitate natural materials to complex systems that reproduce the functionality of biological organs or organisms. Notably, among these biomimetic devices, OECTs demonstrate the ability to detect and manipulate the electrical activity of biological systems. OECTs achieve this by accurately mimicking the ion-driven processes and dynamics observed in biological systems, thereby enabling them to emulate the behavior of artificial neurons, synapses, e-skin, and e-plant systems.^{132,133} In this section, our primary focus lies on OECT-based biosensors that strive to mimic the intricate functions of neurons, synapses, skin, and plant interfacing, with potential applications in fields such as robotics, brain-computer interaction, and regulation of plant function.^{133,134}

Neuromorphic devices

The human brain consists of 10^{11} neurons that are connected through 10^{15} synapses to form a densely interconnected neural network, which operates in parallel to support all brain functions.^{135,136} Neuromorphic devices are bioinspired systems that aim to mimic the parallel signal-processing capability of the brain, enabling applications such as movement control, speech recognition, and visual information processing.^{7,137,138} In prosthetics or robotics applications, thousands of sensing elements generate massive signals that need to be processed simultaneously without interference.¹³⁹ Neuromorphic devices provide compact, fault-tolerant, and energy-efficient solutions for solving complex real-world problems.¹³⁷

Transistor-based artificial synapses have emerged as a promising approach for the development of neuromorphic devices, owing to their unique advantages in terms of wearability, biocompatibility, reconfigurability, and implantability.^{140–142} However, current neuromorphic devices rely on detecting local electric fields generated by synaptic currents and action potentials, which is different from the primary signaling mechanism in biological systems. In biological systems, chemical signaling through neurotransmitter release into the synapse plays a critical role in establishing and modulating synaptic weight. Therefore, to achieve accurate emulation of biological synaptic behavior, the connectivity of artificial synapses must be dynamically regulated based on the local neurotransmitter activity in a manner similar to that occurring in biological synapses. Biohybrid synaptic OECTs represent a promising approach for achieving this goal. Keene et al. developed biohybrid synaptic OECTs by seeding a dopaminergic presynaptic domain of PC-12 cells onto the device to create a presynaptic terminal.¹⁴³ In biohybrid synaptic OECTs, the oxidation of dopamine secreted by the PC-12 cells causes a change in the charge state of the gate electrode, which can regulate the conductance of the device and modulate the synaptic weight. The flow rates in the microfluidic channel can be controlled to emulate the dopamine recycling process in biological synapses, further enhancing the biohybrid device's ability to mimic the plasticity of biological synapses, such as long-term potentiation and long-term depression (LTD) (Figure 12A). The capability of regulating synaptic weights in biohybrid synaptic OECTs has great potential for the development of neuromorphic-based prosthetics. Short-term plasticity in the brain, which plays a critical role in many cognitive processes including sensory processing, memory formation, and attention, can be studied using a biomembrane-based OECT.¹⁴⁴ An ionic barrier in the form of supported lipid bilayers in the membrane of synaptic OECTs hinders ion passage and modulates conductance, allowing analysis of short-term depressive (STD) behavior.

Precise emulation of the spiking and firing behaviors of biological neurons is essential for developing artificial systems or models that mimic their behavior. OECTs have been employed for the creation of artificial neurons because of their ionic-to-electronic transduction, low operation voltage, and flexibility.^{148,145} Harikesh et al. have developed a novel spiking organic electrochemical neuron (OECN) with a leaky integrate and fire type circuit that can mimic spiking neural networks using all-printed complementary OECTs, including a p-type P(g42T-T)-based OECT and an n-type poly(benzimidazobenzophenanthroline) (BBL)-based OECT (Figure 12B).¹³² The device displayed both STD and LTD spiking behaviors that are similar to those of biological neurons, which could facilitate Hebbian learning. Additionally, when coupled with a Venus Flytrap, the device was able to induce electrical stimuli to control the plant's opening and closure, demonstrating the potential for building connections between soft neuromorphic devices and various biointerfaces. They also created a complementary OECN (c-OECN) using channel material based solely on BBL, which included one Na⁺-based OECT and one K⁺-based OECT, each connected to a voltage source. This design was inspired by the activated and inactivated states of the voltage-gated sodium channel in the Hodgkin-Huxley neuron model. To evaluate the c-OECN's potential as a therapeutic intervention, it was coupled with a mouse's right cervical vagus nerve, and the resulting physiological effects and underlying mechanisms of vagus nerve stimulation were analyzed. The experiment revealed a 4.5% decrease in heart rate, which occurred because of the increase in Na⁺ concentration and was consistent with nervous electrical activation (Figure 12C).

More recently, a compact organic artificial spiking neuron (OAN) was developed using a depletion-mode OECT based on a PEDOT:PSS channel and an

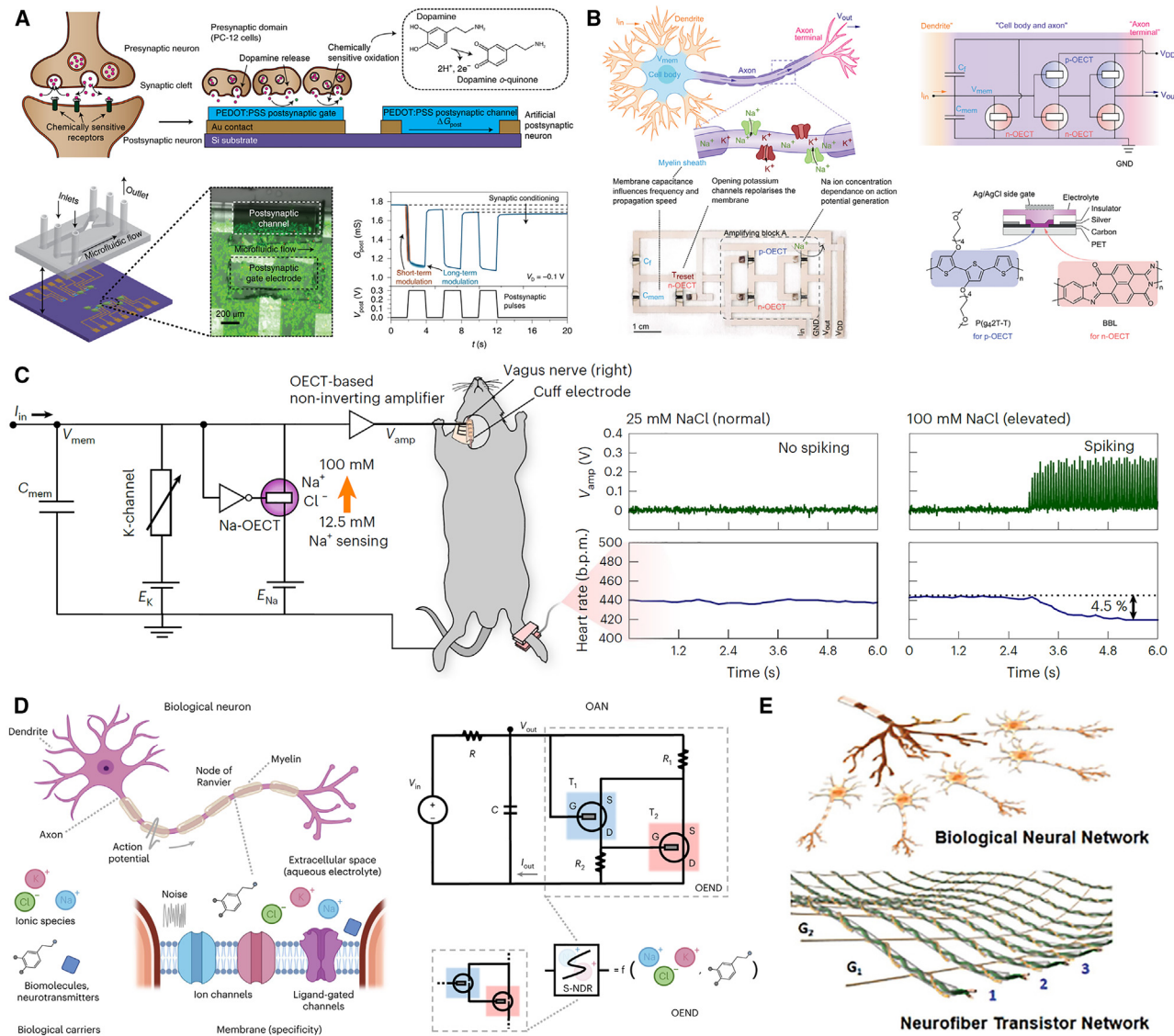


Figure 12. Schematic diagrams of neuromorphic devices composed of OECTs

- (A) Biohybrid synaptic OECTs with P-12 cells seeding. Reproduced with permission from Keene et al.¹⁴³ Copyright 2020, Springer Nature.
- (B) Schematic of a spiking OECN, including p-type-based OECTs and n-type-based OECTs. Reproduced with permission Harikesh et al.¹³² Copyright 2022, Springer Nature.
- (C) The c-OECT circuits coupled with a mouse's right cervical vagus nerve and the corresponding heart rate variations with the concentration of Na^+ . Reproduced with permission from Harikesh et al.¹⁴⁵ Copyright 2023, Springer Nature.
- (D) Schematic of a biological OAN and its circuit design. Reproduced with permission from Sarkar et al.¹⁴⁶ Copyright 2022, Springer Nature.
- (E) Schematic of a textile artificial neural network composed of neuromorphic fibrous OECTs. Reproduced with permission of Kim et al.¹⁴⁷ Copyright 2021, Wiley-VCH.

enhancement-mode OECT based on a p(g2T-TT) channel. The two OECTs were connected in a cascade-like configuration with feedback resistors to create the non-linear device, which was then coupled to a resistor-capacitor element to form the OAN (Figure 12D). The OAN exhibited the ability to modulate the amplitude and window of current or voltage oscillations via the adjustment of threshold voltages in both OECTs. The OECTs within the OAN displayed a high-frequency response to polyatomic ions and ionic species, demonstrating dopamine-mediated spiking response and ion-specific oscillations. Furthermore, the device's capability for

density integration and variability of soft matter was demonstrated by incorporating organic synaptic transistors.¹⁴⁶

Fiber-based OECTs have also shown potential for use in neuromorphic devices.¹⁴⁷ The neuromorphic fibrous OECT was constructed using a double-stranded assembly of electrode microfibers (DSA microfibers) and an ion-gel electrolyte. Specifically, P3HT and P3CT semiconductors were coated on the Au microfiber and twisted into the DSA microfibers. The neuromorphic fibrous OECT based on P3CT exhibited reversible redox reactions in the channel area, resulting in excellent cyclic endurance and stable long-term memory. A textile artificial neural network was created through 20 intercrossed neuromorphic fibrous OECTs (Figure 12E), which can operate with distinct memory states in speech recognition and enhance cyclic memory endurance for spatiotemporal iterative learning. Fiber-based neuromorphic devices are deformable and adaptive electronic components for future smart wearable electronics. The development of fiber-based neuromorphic organic transistors is a crucial step toward a textile artificial neural network capable of neuromorphic computing.

The advancement of synaptic transistors could improve the adaptive control of physiology and processes to nerves, cells, tissues, and organs.^{136,137,149} However, some challenges need to be addressed. First, the working mechanisms of synaptic transistors, such as potential switching, transmission, and conducting path formation, require further exploration. Second, the conductivity and mobility of organic semiconductors need improvement to enhance energy efficiency, device stability, and cycling endurance in real applications. Third, the implementation of massive synaptic transistors interconnected to form a brain-like neural network remains to be realized. Fourth, the current limited understanding of brain function limits the development of neuromorphic devices.

E-skin

The integration of intrinsically stretchable OECTs with pressure and temperature sensors provides an opportunity to emulate the temperature/toughness/pressure capability of the human skin. This integration allows for the identification and quantification of precise sensing signals from mechanical or thermal stimuli, which is crucial for human health monitoring and e-skin development. Recently, numerous strategies have been developed to obtain intrinsically stretchable thin-film devices for emerging wearable electronics and soft bioelectronic e-skin. For example, Liu et al. fabricated intrinsically stretchable OECTs by employing elastic thermoplastic polyurethane (TPU) substrates with extremely low oxygen permeability (Figure 13A).¹⁵⁰ The resulting intrinsically stretchable OECTs exhibited a record-high on/off ratio ($\sim 10^4$) and mobility retention ($\sim 1.1 \text{ cm}^2 \text{ V}^{-1} \cdot \text{s}^{-1}$) even after being stretched up to 50%. Notably, the PEDOT:PSS film integrated onto TPU substrates exhibited minimal cracking at 50% strain due to the favorable Young's modulus match, eliminating the need for additional plasticizers and improving the potential for commercialization.

Mechanical breakdown can significantly reduce the practicality and longevity of e-skin applications, as it can result from factors such as wear, tear, mechanical stress, temperature changes, and moisture exposure. To enhance the intrinsic stretchability and durability of e-skin a self-healable conducting polymer has been developed, which comprises a conductive polymer, PEDOT:PSS, a soft polymeric material, poly(2-acrylamido-2-methyl-1-propanesulfonic acid) (PAMPS), and an ionic liquid, 1-ethyl-3-methylimidazolium trifluoromethanesulfonate (EMIM OTF).¹⁵¹ This

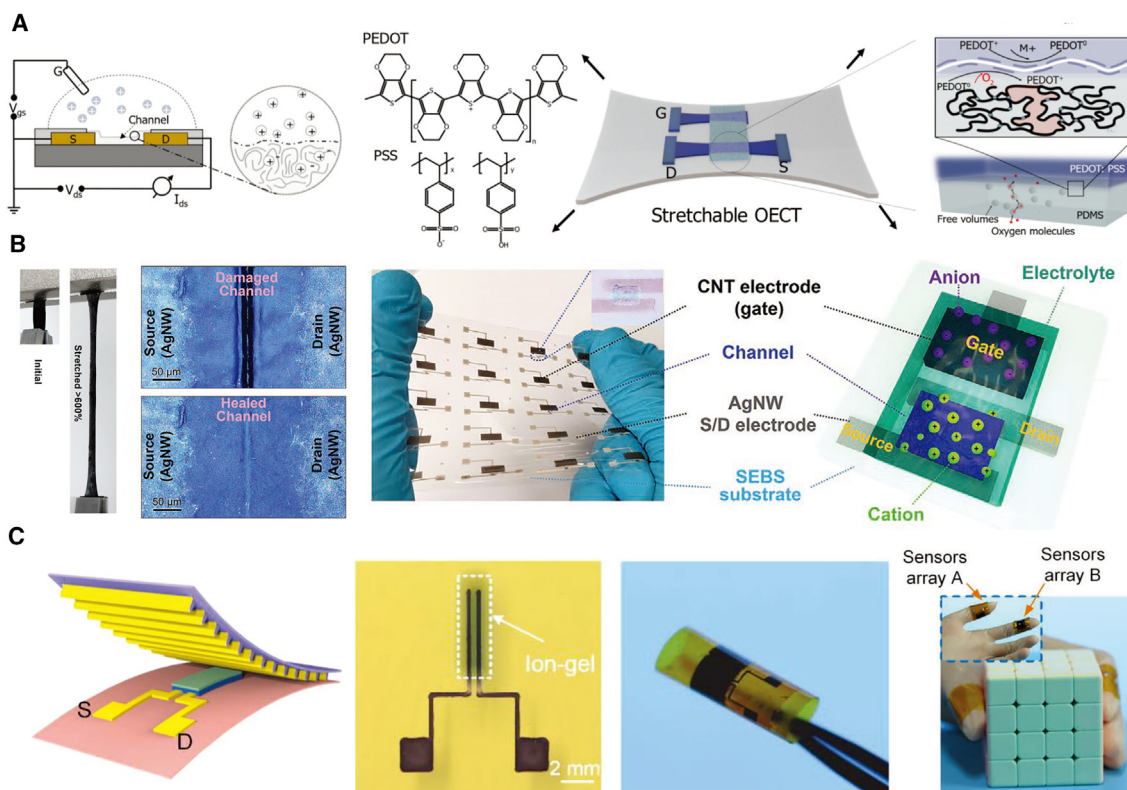


Figure 13. The potential use of flexible OECTs in e-skin applications

(A) Schematic diagrams of stretchable OECTs with potential applications in e-skin. Reproduced with permission from Liu et al.¹⁵⁰ Copyright 2022, Wiley-VCH.

(B) Stretchable OECT arrays with self-healable channel for tactile sensing. Reproduced with permission from Su et al.¹⁵¹ Copyright 2022, Wiley-VCH.

(C) Ultra-flexible OECTs printed via aerosol jet technology for sensing grabbing forces and recognizing states. Reproduced with permission from Zhou et al.¹³⁴ Copyright 2023, Wiley-VCH.

stretchable film can maintain high electrical conductivity even when subjected to strains exceeding 600%, and it is capable of repairing damaged areas caused by both mechanical and electrical breakdowns (Figure 13B). This is due to the hydrogen and ionic bonds that form between PEDOT:PSS and PAMPS, which undergo an energy dissipation mechanism when exposed to strain or severe mechanical damage. The damaged bonds can then be reformed to restore the material's mechanical properties. Moreover, the stretchable polymer composite film has been demonstrated to be suitable for use in e-skin applications requiring high stretchability and reliability, such as tactile sensing. The stretchable OECT array fabricated using this material exhibited outstanding pressure sensitivity, ultra-fast response time, and impressive endurance. These properties make the stretchable polymer composite film a promising candidate for use in various e-skin applications, where it can improve the material's stretchability, durability, and reliability.

Soft bump structures have been utilized in e-skin applications for tactile and force sensing by detecting the directional deformations of bumps, mimicking the interlocked dermis-epidermis interface found in human skin.¹⁵² However, miniaturizing this structure is challenging, and irregular skin attachment is limited by the size of the sensing electrodes and the lack of high-deposition precision technology. To address these limitations, Zhou et al. developed an ultra-thin, deformable, multi-dimensional tactile sensor based on OECT technology (Figure 13C).¹³⁴ The OECT

force sensor, which comprises a micro-riblets array structure gate electrode and OECT sensing layer, was fabricated using aerosol jet printing with accurate pattern depositing techniques. The sensor features a unilateral conductive micro-riblets array, enabling tunable range and sensitivity, and the device exhibits adjustable sensing performance, with high sensitivity of approximately 1.45 kPa^{-1} in the low-pressure range (0–500 Pa) and a large measuring range of up to 50 kPa. Furthermore, the sensor can be used for force sensing and state recognition during grasping by bonding it to human or robotic fingers (Figure 13C). This technology has potential applications in intelligent robotics and human-machine interaction.

E-plants

The root and shoot systems of higher plants serve as an intricate communication network, exhibiting similarities to electronic circuits, and play a vital role in transmitting chemical signals that govern growth and various physiological functions. These signals are influenced by environmental factors, such as light and temperature, as well as hormones, and nutrients present in the plant's surroundings. They propagate through the xylem and phloem vascular systems, serving as conduits, to initiate and modulate processes within the plant. However, owing to the intricacy and spatio-temporal dynamics of these processes, there is an urgent requirement to precisely record, address, and locally regulate plant functions.¹⁵³

In response to this need, the integration of OECT technology into living plants has emerged as a promising solution for the local regulation of plant functions. Notably, researchers have successfully developed OECT circuits within the xylem and leaves of living roses, enabling precise control over the plant's energy harvest from photosynthesis.¹⁵³ This integration allows for modulation and optimization of the plant's energy utilization, thereby promoting efficient growth and physiological processes. Similarly, OECT biosensors have been seamlessly incorporated into tomato plants, facilitating continuous monitoring of various physiological parameters. These biosensors can track ion concentration in the sap during drought conditions,¹⁵⁴ saturation levels,¹⁵⁵ and variations in solute content of the plant sap.¹⁵⁶ Real-time monitoring capability provides valuable insights into the plant's physiological status and responses to environmental changes. In the case of diurnal sugar homeostasis monitoring in trees, OECTs have been implanted into the vascular tissue of hybrid aspen trees to achieve continuous measurement of sucrose and glucose levels.¹⁵⁷ This ongoing monitoring of sugar levels not only allows for real-time assessment of plant metabolites influenced by surrounding biotic environment but also provides valuable insights across various disciplines, including plant science and genetic science. Additionally, the utilization of OECT technology has facilitated the measurement of plant action potentials¹⁵⁸ as well as the assessment of plant nutritional levels.¹⁵⁹ These advancements have shed light on the electrical signaling mechanisms that underlie plants' sensory capabilities.

The integration of OECT technology into living plants represents a significant step forward in understanding and manipulation of plant physiology. By leveraging these advancements, researchers can achieve highly complex and spatiotemporally resolved recordings and regulation of plant functions. This breakthrough carries extensive implications across various disciplines, including agriculture, horticulture, and ecological studies, as it empowers the precise management of crop productivity, stress responses, and sustainable farming practices. The integration of OECTs into plants opens up new avenues for scientific exploration and innovation, allowing for a deeper comprehension of the intricate processes underlying plant growth and development.

CONCLUSION AND OUTLOOK

In conclusion, this comprehensive and timely review aims to contribute to the advancement of higher-performance flexible biosensors for diverse functional applications. Flexible OECTs have demonstrated great potential for biosensing applications both *in vivo* and *in vitro*. These applications encompass the acquisition of physiological information, monitoring of electrophysiological processes, assessing cell activity, and detecting ions, metabolites, nucleic acids, and proteins. OECTs have also been employed in neuromorphic devices and e-skin thanks to their unique properties, including high sensitivity, biocompatibility, and flexibility. The functionalization of OECTs with different sensing materials through the channel layers, gate electrodes, and electrolyte has enabled the creation of biosensors that can detect various health conditions in real time, including various body fluids, biomolecules, and ionic solutions, with high selectivity and specificity.

One of the key advantages of flexible OECTs for biosensing is their ability to conform to the surface of the body and organs. This characteristic makes them highly suitable for applications involving stretchable, wearable, and implantable devices (Figure 14B). Moreover, their ease of use in household settings, along with the potential integration with the future Mobile Internet of Things ecosystem, such as smartphones, smart glasses, and smart watches (Figure 14A), positions them to significantly contribute to point-of-care testing and personalized medicine. These adaptable devices can be used for continuous and personalized monitoring of various health conditions, including non-invasive glucose levels in diabetic patients or electrocardiographic signals, blood pressure, and oxygen saturation in individuals with cardiovascular diseases. In addition, the development of intrinsically stretchable OECTs has opened up new opportunities for the creation of e-skin, capable of withstanding the mechanical stresses imposed by the body (Figure 14C). The data obtained from the OECT sensing platform can be analyzed using artificial intelligence algorithms and transmitted to mobile devices for recording and analysis (Figure 14D). This integration of advanced technologies has the potential to revolutionize disease management and bioelectronics, providing valuable insights into the development and treatment of various medical conditions.

Nonetheless, there are still challenges that need to be addressed in the field, such as the innovation of OMIEC materials and the optimization of sensing performance. Personalized OMIECs, which establish a relationship between microstructure and properties, could enhance the performance of OECTs. Recent attention has been given to 2D polymers and MOFs because of their ordered porous microstructures, which enable efficient ion and charge-carrier transport, leading to high-performance OECTs.³⁶ Additionally, the architecture of innovative devices can also enhance the behavior and stability of transistors, with ion-impermeable contacts enabling the achievement of vertical OECTs throughout the entire semiconductor bulk. Short channels provide these devices with high transconductance, low driving voltage, low power consumption, and fast response time, making them attractive for diverse biosensing applications.¹⁷

In practical trials, significant efforts are being made to address the stability, reproducibility, and integration of OECTs with other electronic components. The objective is to ensure consistent performance at intended levels and seamless integration. To effectively deploy OECTs in practical trials, such as wearable bioinformatics analysis and biological signal acquisition *in vivo* and *in vitro*, it is crucial to consider the potential impact of various environmental factors on the properties of organic

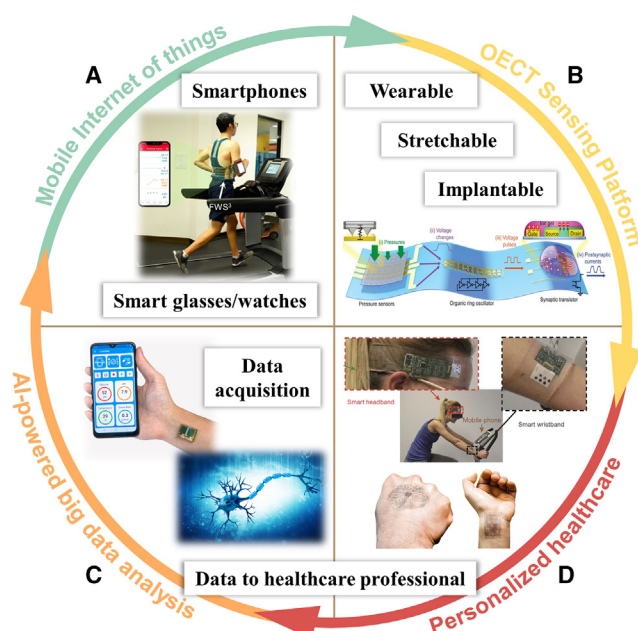


Figure 14. Schematic illustration of healthcare application utilizing OECT

(A) Mobile Internet of Things for OECT technology. Reproduced with permission from Song et al.¹⁶⁰ Copyright 2020, AAAS.

(B) OECT sensing platform. Reproduced with permission from Kim et al.¹³⁷ Copyright 2018, AAAS.

(C) Personalized healthcare. Images of sweat sensors were reproduced with permission from Gao et al.¹⁶¹ Copyright 2016, Springer Nature. Images of e-skin were reproduced with permission from Jiang et al.¹⁶² Copyright 2022, AAAS.

(D) AI-powered big data analysis. Data acquisition using smartphone was reproduced with permission from Min et al.¹⁶³ Copyright 2023, Springer Nature. Image of synapse was reproduced with permission from Waltz.¹⁶⁴ Copyright 2016, Springer Nature.

materials and biorecognition elements. Environmental factors such as chemicals, temperature, air, water, noise, light, acidity, and alkalinity can influence the performance and longevity of these devices. Researchers are conducting chronic stability testing and implementing systematic characterizations to investigate degradation mechanisms and provide valuable insights for the development of robust biosensors capable of withstanding diverse environmental conditions. By improving the lifetime and long-term stability of OECTs, their commercialization for real medical devices can be enhanced. This is an important step toward ensuring the reliability and functionality of these devices, enabling their successful integration into practical applications.

Despite these challenges, the future outlook for flexible OECTs in biosensing is promising. The development of such devices could lead to personalized healthcare and improved patient outcomes. With ongoing research and development, flexible OECTs have the potential to revolutionize the field of biosensing, enabling the creation of wearable and implantable devices that can monitor and diagnose various health conditions in real time.

ACKNOWLEDGMENTS

This study received support from multiple sources, including the Research Institute of Intelligent Wearable Systems (project code: CD46) and the Research Institute for Sports Science and Technology (project code: CD6X) of the Hong Kong Polytechnic

University, as well as the Projects of Strategic Importance (project code: 1-ZE2X) of the same institution.

AUTHOR CONTRIBUTIONS

Conceptualization, Z.Z. and F.Y.; investigation, Z.Z. and Z.T.; writing – original draft, Z.Z.; writing – review & editing, Z.Z. and F.Y.; supervision, F.Y.; funding acquisition, F.Y.

DECLARATION OF INTERESTS

The authors declare no competing interests.

REFERENCES

- Turner, A.P.F. (2013). Biosensors: sense and sensibility. *Chem. Soc. Rev.* 42, 3184–3196. <https://doi.org/10.1039/C3CS35528D>.
- Liao, C., Zhang, M., Yao, M.Y., Hua, T., Li, L., and Yan, F. (2015). Flexible organic electronics in biology: materials and devices. *Adv. Mater.* 27, 7493–7527. <https://doi.org/10.1002/adma.201402625>.
- Berggren, M., and Richter-Dahlfors, A. (2007). Organic bioelectronics. *Adv. Mater.* 19, 3201–3213. <https://doi.org/10.1002/adma.200700419>.
- Ohayon, D., and Inal, S. (2020). Organic bioelectronics: from functional materials to next-generation devices and power sources. *Adv. Mater.* 32, 2001439. <https://doi.org/10.1002/adma.202001439>.
- Simon, D.T., Gabrielsson, E.O., Tybrandt, K., and Berggren, M. (2016). Organic bioelectronics: bridging the signaling gap between biology and technology. *Chem. Rev.* 116, 13009–13041. <https://doi.org/10.1021/acs.chemrev.6b00146>.
- Hong, G., Gan, X., Leonhardt, C., Zhang, Z., Seibert, J., Busch, J.M., and Bräse, S. (2021). A brief history of OLEDs—emitter development and industry milestones. *Adv. Mater.* 33, 2005630. <https://doi.org/10.1002/adma.202005630>.
- Yang, J.C., Mun, J., Kwon, S.Y., Park, S., Bao, Z., and Park, S. (2019). Electronic skin: recent progress and future prospects for skin-attachable devices for health monitoring, robotics, and prosthetics. *Adv. Mater.* 31, 1904765. <https://doi.org/10.1002/adma.201800051>.
- Rivnay, J., Inal, S., Salleo, A., Owens, R.M., Berggren, M., and Malliaras, G.G. (2018). Organic electrochemical transistors. *Nat. Rev. Mater.* 3, 17086. <https://doi.org/10.1038/natrevmats.2017.86V>.
- Lin, P., and Yan, F. (2012). Organic thin-film transistors for chemical and biological sensing. *Adv. Mater.* 24, 34–51. <https://doi.org/10.1002/adma.201103334>.
- Torsi, L., Magliulo, M., Manoli, K., and Palazzo, G. (2013). Organic field-effect transistor sensors: a tutorial review. *Chem. Soc. Rev.* 42, 8612–8628. <https://doi.org/10.1039/C3CS60127G>.
- Horowitz, G. (1998). Organic field-effect transistors. *Adv. Mater.* 10, 365–377. [https://doi.org/10.1002/\(SICI\)1521-4095\(199803\)10:5<365::AID-ADMA365>3.0.CO;2-U](https://doi.org/10.1002/(SICI)1521-4095(199803)10:5<365::AID-ADMA365>3.0.CO;2-U).
- Kim, S.H., Hong, K., Xie, W., Lee, K.H., Zhang, S., Lodge, T.P., and Frisbie, C.D. (2013). Electrolyte-gated transistors for organic and printed electronics. *Adv. Mater.* 25, 1822–1846. <https://doi.org/10.1002/adma.201202790>.
- Sun, C., Wang, X., Auwalu, M.A., Cheng, S., and Hu, W. (2021). Organic thin film transistors-based biosensors. *EcoMat* 3. <https://doi.org/10.1002/eom2.12094>.
- Roberts, M.E., Mannsfeld, S.C.B., Tang, M.L., and Bao, Z. (2008). Influence of molecular structure and film properties on the water-stability and sensor characteristics of organic transistors. *Chem. Mater.* 20, 7332–7338. <https://doi.org/10.1021/cm802530x>.
- Smela, E. (2003). Conjugated polymer actuators for biomedical applications. *Adv. Mater.* 15, 481–494. <https://doi.org/10.1002/adma.200390113>.
- Minamiki, T., Tokito, S., and Minami, T. (2019). Fabrication of a flexible biosensor based on an organic field-effect transistor for lactate detection. *Anal. Sci.* 35, 103–106. <https://doi.org/10.2116/analsci.18SDN02>.
- Huang, W., Chen, J., Yao, Y., Zheng, D., Ji, X., Feng, L.-W., Moore, D., Glavin, N.R., Xie, M., Chen, Y., et al. (2023). Vertical organic electrochemical transistors for complementary circuits. *Nature* 613, 496–502. <https://doi.org/10.1038/s41586-022-05592-2>.
- Dai, Y., Dai, S., Li, N., Li, Y., Moser, M., Strzalka, J., Prominski, A., Liu, Y., Zhang, Q., Li, S., et al. (2022). Stretchable redox-active semiconducting polymers for high-performance organic electrochemical transistors. *Adv. Mater.* 34, 2201178. <https://doi.org/10.1002/adma.202201178>.
- Wustoni, S., Combe, C., Ohayon, D., Akhtar, M.H., McCulloch, I., and Inal, S. (2019). Membrane-free detection of metal cations with an organic electrochemical transistor. *Adv. Funct. Mater.* 29, 1904403. <https://doi.org/10.1002/adfm.201904403>.
- Wang, S., Xu, J., Wang, W., Wang, G.-J.N., Rastak, R., Molina-Lopez, F., Chung, J.W., Niu, S., Feig, V.R., Lopez, J., et al. (2018). Skin electronics from scalable fabrication of an intrinsically stretchable transistor array. *Nature* 555, 83–88. <https://doi.org/10.1038/nature25494>.
- Zheng, Y.-Q., Liu, Y., Zhong, D., Nikzad, S., Liu, S., Yu, Z., Liu, D., Wu, H.-C., Zhu, C., Li, J., et al. (2021). Monolithic optical microlithography of high-density elastic circuits. *Science* 373, 88–94. <https://doi.org/10.1126/science.abh3551>.
- Wang, J., Ye, D., Meng, Q., Di, C.-a., and Zhu, D. (2020). Advances in organic transistor-based biosensors. *Adv. Mater. Technol.* 5, 2000218. <https://doi.org/10.1002/admt.202000218>.
- Bernards, D., and Malliaras, G. (2007). Steady-state and transient behavior of organic electrochemical transistors. *Adv. Funct. Mater.* 17, 3538–3544. <https://doi.org/10.1002/adfm.200601239>.
- Khodagholy, D., Rivnay, J., Sessolo, M., Gurfinkel, M., Leleux, P., Jimison, L.H., Stavriniidou, E., Herve, T., Sanaur, S., Owens, R.M., and Malliaras, G.G. (2013). High transconductance organic electrochemical transistors. *Nat. Commun.* 4, 2133. <https://doi.org/10.1038/ncomms3133>.
- Ohayon, D., Druet, V., and Inal, S. (2023). A guide for the characterization of organic electrochemical transistors and channel materials. *Chem. Soc. Rev.* 52, 1001–1023. <https://doi.org/10.1039/D2CS00920J>.
- Cendra, C., Giovannitti, A., Savva, A., Venkatraman, V., McCulloch, I., Salleo, A., Inal, S., and Rivnay, J. (2019). Role of the anion on the transport and structure of organic mixed conductors. *Adv. Funct. Mater.* 29, 1807034. <https://doi.org/10.1002/adfm.201807034>.
- Zeglio, E., Eriksson, J., Gabrielsson, R., Solin, N., and Inganäs, O. (2017). Highly stable conjugated polyelectrolytes for water-based hybrid mode electrochemical transistors. *Adv. Mater.* 29, 1605787. <https://doi.org/10.1002/adma.201605787>.
- Song, J., Liu, H., Zhao, Z., Lin, P., and Yan, F. (2023). Flexible organic transistors for biosensing: devices and applications. *Adv. Mater.* 2300034. <https://doi.org/10.1002/adma.202300034>.
- Tian, X., Liu, D., Bai, J., Chan, K.S., Ip, L.C., Chan, P.K.L., and Zhang, S. (2022). Pushing OECTs toward wearable development of a miniaturized analytical control unit for

- wireless device characterization. *Anal. Chem.* 94, 6156–6162. <https://doi.org/10.1021/acs.analchem.1c05210>.
30. Chen, S., Surendran, A., Wu, X., and Leong, W.L. (2020). Contact modulated ionic transfer doping in all-solid-state organic electrochemical transistor for ultra-high sensitive tactile perception at low operating voltage. *Adv. Funct. Mater.* 30, 2006186. <https://doi.org/10.1002/adfm.202006186>.
31. Song, J., Tang, G., Cao, J., Liu, H., Zhao, Z., Griggs, S., Yang, A., Wang, N., Cheng, H., Liu, C.-K., et al. (2023). Perovskite solar cell-gated organic electrochemical transistors for flexible photodetectors with ultrahigh sensitivity and fast response. *Adv. Mater.* 35, 2207763. <https://doi.org/10.1002/adma.202207763>.
32. Park, S., Heo, S.W., Lee, W., Inoue, D., Jiang, Z., Yu, K., Jinno, H., Hashizume, D., Sekino, M., Yokota, T., et al. (2018). Self-powered ultra-flexible electronics via nano-grating-patterned organic photovoltaics. *Nature* 561, 516–521. <https://doi.org/10.1038/s41586-018-0536-x>.
33. Lee, H., Lee, S., Lee, W., Yokota, T., Fukuda, K., and Someya, T. (2019). Ultrathin organic electrochemical transistor with nonvolatile and thin gel electrolyte for long-term electrophysiological monitoring. *Adv. Funct. Mater.* 29, 1906982. <https://doi.org/10.1002/adfm.201906982>.
34. Wang, J., Lee, S., Yokota, T., and Someya, T. (2022). Gas-permeable organic electrochemical transistor embedded with a porous solid-state polymer electrolyte as an on-skin active electrode for electrophysiological signal acquisition. *Adv. Funct. Mater.* 32, 2200458. <https://doi.org/10.1002/adfm.202200458>.
35. Lee, W., Kobayashi, S., Nagase, M., Jimbo, Y., Saito, I., Inoue, Y., Yambe, T., Sekino, M., Malliaras, G.G., Yokota, T., et al. (2018). Nonthrombogenic, stretchable, active multielectrode array for electroanatomical mapping. *Sci. Adv.* 4, eaau2426. <https://doi.org/10.1126/sciadv.aau2426>.
36. Song, J., Liu, H., Zhao, Z., Guo, X., Liu, C.K., Griggs, S., Marks, A., Zhu, Y., Law, H.K.-w., McCulloch, I., and Yan, F. (2023). 2D metal-organic frameworks for ultraflexible electrochemical transistors with high transconductance and fast response speeds. *Sci. Adv.* 9, add9627. <https://doi.org/10.1126/sciadv.add9627>.
37. Chen, J., Huang, W., Zheng, D., Xie, Z., Zhuang, X., Zhao, D., Chen, Y., Su, N., Chen, H., Pankow, R.M., et al. (2022). Highly stretchable organic electrochemical transistors with strain-resistant performance. *Nat. Mater.* 21, 564–571. <https://doi.org/10.1038/s41563-022-01239-9>.
38. Cea, C., Spyropoulos, G.D., Jastrzebska-Perfect, P., Ferrero, J.J., Gelinas, J.N., and Khodagholy, D. (2020). Enhancement-mode ion-based transistor as a comprehensive interface and real-time processing unit for in vivo electrophysiology. *Nat. Mater.* 19, 679–686. <https://doi.org/10.1038/s41563-020-0638-3>.
39. Yao, Y., Huang, W., Chen, J., Wang, G., Chen, H., Zhuang, X., Ying, Y., Ping, J., Marks, T.J., and Facchetti, A. (2021). Flexible complementary circuits operating at sub-0.5 V via hybrid organic inorganic electrolyte-gated transistors. *Proc. Natl. Acad. Sci. USA* 118, e2111790118. <https://doi.org/10.1073/pnas.2111790118>.
40. Spyropoulos, G.D., Gelinas, J.N., and Khodagholy, D. (2019). Internal ion-gated organic electrochemical transistor: A building block for integrated bioelectronics. *Sci. Adv.* 5, eaau7378. <https://doi.org/10.1126/sciadv.aau7378>.
41. Wu, M., Yao, K., Huang, N., Li, H., Zhou, J., Shi, R., Li, J., Huang, X., Li, J., Jia, H., et al. (2023). Ultrathin, soft, bioresorbable organic electrochemical transistors for transient spatiotemporal mapping of brain activity. *Adv. Sci.* 10, 2300504. <https://doi.org/10.1002/advs.202300504>.
42. Pitsalidis, C., Ferro, M.P., Iandolo, D., Tzounis, L., Inal, S., and Owens, R.M. (2018). Transistor in a tube: A route to three-dimensional bioelectronics. *Sci. Adv.* 4, eaat4253. <https://doi.org/10.1126/sciadv.aat4253>.
43. Decataldo, F., Barbalinardo, M., Tassarolo, M., Vurro, V., Calieni, M., Gentili, D., Valle, F., Cavallini, M., and Fraboni, B. (2019). Organic electrochemical transistors: smart devices for real-time monitoring of cellular vitality. *Adv. Mater. Technol.* 4, 1900207. <https://doi.org/10.1002/admt.201900207>.
44. Decataldo, F., Grumiro, L., Marino, M.M., Faccin, F., Giovannini, C., Brandolini, M., Dirani, G., Taddei, F., Lelli, D., Tassarolo, M., et al. (2022). Fast and real-time electrical transistor assay for quantifying SARS-CoV-2 neutralizing antibodies. *Commun. Mater.* 3, 5–9. <https://doi.org/10.1038/s43246-022-00226-6>.
45. Gu, X., Yeung, S.Y., Chadda, A., Poon, E.N.Y., Boheler, K.R., and Hsing, I.M. (2019). Organic electrochemical transistor arrays for in vitro electrophysiology monitoring of 2d and 3d cardiac tissues. *Adv. Biosyst.* 3, 1800248. <https://doi.org/10.1002/adbi.201800248>.
46. Decataldo, F., Barbalinardo, M., Gentili, D., Tassarolo, M., Calieni, M., Cavallini, M., and Fraboni, B. (2020). Organic electrochemical transistors for real-time monitoring of in vitro silver nanoparticle toxicity. *Adv. Biosyst.* 4, 1900204. <https://doi.org/10.1002/adbi.201900204>.
47. Abarkan, M., Pirog, A., Mafila, D., Pathak, G., N'Kaoua, G., Puginier, E., O'Connor, R., Raoux, M., Donahue, M.J., Renaud, S., and Lang, J. (2022). Vertical Organic Electrochemical Transistors and Electronics for Low Amplitude Micro-Organ Signals. *Adv. Sci.* 9, 2105211. <https://doi.org/10.1002/advs.202105211>.
48. Liang, Y., Ernst, M., Brings, F., Kireev, D., Maybeck, V., Offenhäusser, A., and Mayer, D. (2018). High performance flexible organic electrochemical transistors for monitoring cardiac action potential. *Adv. Healthcare Mater.* 7, 1800304. <https://doi.org/10.1002/adhm.201800304>.
49. Bonafé, F., Decataldo, F., Zironi, I., Remondini, D., Cramer, T., and Fraboni, B. (2022). AC amplification gain in organic electrochemical transistors for impedance-based single cell sensors. *Nat. Commun.* 13, 1–9. <https://doi.org/10.1038/s41467-022-33094-2>.
50. Hempel, F., Law, J.K.Y., Nguyen, T.C., Lanche, R., Susloparova, A., Vu, X.T., and Ingebrandt, S. (2021). PEDOT:PSS organic electrochemical transistors for electrical cell-substrate impedance sensing down to single cells. *Biosens. Bioelectron.* 180, 113101. <https://doi.org/10.1016/j.bios.2021.113101>.
51. Chen, L., Fu, Y., Wang, N., Yang, A., Li, Y., Wu, J., Ju, H., and Yan, F. (2018). Organic electrochemical transistors for the detection of cell surface glycans. *ACS Appl. Mater. Interfaces* 10, 18470–18477. <https://doi.org/10.1021/acsami.8b01987>.
52. Frantz, E., Huang, J., Han, D., and Steckl, A.J. (2022). The effect of nutrient broth media on PEDOT: PSS gated OECTs for whole-cell bacteria detection. *Biosens. Bioelectron.* 12, 100268. <https://doi.org/10.1016/j.bios.2022.100268>.
53. Butina, K., Filipovic, F., Richter-Dahlfors, A., and Parlak, O. (2021). An organic electrochemical transistor to monitor salmonella growth in real-time. *Adv. Mater. Interfac.* 8, 2100961. <https://doi.org/10.1002/admi.202100961>.
54. Lin, B., Wang, M., Zhao, C., Wang, S., Chen, K., Li, X., Long, Z., Zhao, C., Song, X., Yan, S., et al. (2022). Flexible organic integrated electronics for self-powered multiplexed ocular monitoring. *Npj Flex. Electron.* 6, 77–78. <https://doi.org/10.1038/s41528-022-00211-6>.
55. Kim, T.H., Kim, H., Kim, I.C., Yoon, H.J., Park, H.S., Cho, Y.K., Nam, C.W., Han, S., Hur, S.H., and Kim, Y.N. (2018). Organic electrochemical transistor-based channel dimension-independent single-strand wearable sweat sensors. *NPG Asia Mater.* 10, 1086–1092. <https://doi.org/10.1038/s41427-018-0097-3>.
56. Li, T., Cheryl Koh, J.Y., Moudgil, A., Cao, H., Wu, X., Chen, S., Hou, K., Surendran, A., Stephen, M., Tang, C., et al. (2022). Biocompatible ionic liquids in high-performing organic electrochemical transistors for ion detection and electrophysiological monitoring. *ACS Nano* 16, 12049–12060. <https://doi.org/10.1021/acsnano.2c02191>.
57. Chen, X., Ji, J., Peng, Y., Gao, Z., Zhao, M., Tang, B., and Liu, Y. (2023). Flexible pH sensors based on OECTs with a BTB dye-embedded ion-gel gate dielectric. *J. Mater. Chem. C* 11, 7722–7731. <https://doi.org/10.1039/D2TC03940K>.
58. Takemoto, A., Araki, T., Nishimura, K., Akiyama, M., Uemura, T., Kiriya, K., Koot, J.M., Kasai, Y., Kurihara, N., Osaki, S., et al. (2023). Fully transparent, ultrathin flexible organic electrochemical transistors with additive integration for bioelectronic applications. *Adv. Sci.* 10, 2204746. <https://doi.org/10.1002/advs.202204746>.
59. Ohayon, D., Nikiforidis, G., Savva, A., Giugni, A., Wustoni, S., Palanisamy, T., Chen, X., Maria, I.P., Di Fabrizio, E., Costa, P.M.F.J., et al. (2020). Biofuel powered glucose

- detection in bodily fluids with an n-type conjugated polymer. *Nat. Mater.* 19, 456–463. <https://doi.org/10.1038/s41563-019-0556-4>.
60. Koklu, A., Ohayon, D., Wustoni, S., Hama, A., Chen, X., McCulloch, I., and Inal, S. (2021). Microfluidics integrated n-type organic electrochemical transistor for metabolite sensing. *Sens. Actuators, B* 329, 129251. <https://doi.org/10.1016/j.snb.2020.129251>.
61. Yang, A., Li, Y., Yang, C., Fu, Y., Wang, N., Li, L., and Yan, F. (2018). Fabric organic electrochemical transistors for biosensors. *Adv. Mater.* 30, 1800051. <https://doi.org/10.1002/adma.201800051>.
62. Wu, X., Feng, J., Deng, J., Cui, Z., Wang, L., Xie, S., Chen, C., Tang, C., Han, Z., Yu, H., et al. (2020). Fiber-shaped organic electrochemical transistors for biochemical detections with high sensitivity and stability. *Sci. China Chem.* 63, 1281–1288. <https://doi.org/10.1007/s11426-020-9779-1>.
63. Qing, X., Chen, H., Zeng, F., Jia, K., Shu, Q., Wu, J., Xu, H., Lei, W., Liu, D., Wang, X., et al. (2023). All-fiber integrated thermoelectrically powered physiological monitoring biosensor. *Adv. Fiber Mater.* 5, 1025–1036. <https://doi.org/10.1007/s42765-023-00258-8>.
64. Diacci, C., Lee, J.W., Janson, P., Dufil, G., Méhes, G., Berggren, M., Simon, D.T., and Stavrinidou, E. (2020). Real-time monitoring of glucose export from isolated chloroplasts using an organic electrochemical transistor. *Adv. Mater. Technol.* 5, 1900262. <https://doi.org/10.1002/admt.201900262>.
65. Pappa, A.M., Ohayon, D., Giovannitti, A., Maria, I.P., Savva, A., Uguz, I., Rivnay, J., McCulloch, I., Owens, R.M., and Inal, S. (2018). Direct metabolite detection with an n-type accumulation mode organic electrochemical transistor. *Sci. Adv.* 4, eaat0911. <https://doi.org/10.1126/sciadv.aat0911>.
66. Zhang, Y., Wang, Y., Qing, X., Wang, Y., Zhong, W., Wang, W., Chen, Y., Liu, Q., Li, M., and Wang, D. (2020). Fiber organic electrochemical transistors based on multi-walled carbon nanotube and polypyrrole composites for noninvasive lactate sensing. *Anal. Bioanal. Chem.* 412, 7515–7524. <https://doi.org/10.1007/s00216-020-02886-0V>.
67. Zhang, L., Wang, G., Wu, D., Xiong, C., Zheng, L., Ding, Y., Lu, H., Zhang, G., and Qiu, L. (2018). Highly selective and sensitive sensor based on an organic electrochemical transistor for the detection of ascorbic acid. *Biosens. Bioelectron.* 100, 235–241. <https://doi.org/10.1016/j.bios.2017.09.006>.
68. Zhu, R., Wang, Y., Tao, Y., Wang, Y., Chen, Y., Li, M., Liu, Q., Yang, L., and Wang, D. (2022). Layer-by-layer assembly of composite conductive fiber-based organic electrochemical transistor for highly sensitive detection of sialic acid. *Electrochim. Acta* 425, 140716. <https://doi.org/10.1016/j.electacta.2022.140716>.
69. Galliani, M., Diacci, C., Berto, M., Sensi, M., Beni, V., Berggren, M., Borsari, M., Simon, D.T., Biscarini, F., and Bortolotti, C.A. (2020). Flexible printed organic electrochemical transistors for the detection of uric acid in artificial wound exudate. *Adv. Mater. Interfac.* 7, 2001218. <https://doi.org/10.1002/admi.2001218>.
70. Aerathupalathu Janardhanan, J., Chen, Y.-L., Liu, C.-T., Tseng, H.-S., Wu, P.-I., She, J.-W., Hsiao, Y.-S., and Yu, H.-h. (2022). Sensitive detection of sweat cortisol using an organic electrochemical transistor featuring nanostructured poly (3, 4-ethylenedioxythiophene) derivatives in the channel layer. *Anal. Chem.* 94, 7584–7593. <https://doi.org/10.1021/acs.analchem.2c00497>.
71. Parlak, O., Keene, S.T., Marais, A., Curto, V.F., and Salteo, A. (2018). Molecularly selective nanoporous membrane-based wearable organic electrochemical device for noninvasive cortisol sensing. *Sci. Adv.* 4, eaar2904. <https://doi.org/10.1126/sciadv.aar2904>.
72. Demuru, S., Kim, J., El Chazli, M., Bruce, S., Dupertuis, M., Binz, P.A., Saubade, M., Lafaye, C., and Briand, D. (2022). Antibody-Coated Wearable Organic Electrochemical Transistors for Cortisol Detection in Human Sweat. *ACS Sens.* 7, 2721–2731. <https://doi.org/10.1021/acssensors.2c01250>.
73. Fenoy, G.E., von Bilderling, C., Knoll, W., Azzaroni, O., and Marmisollé, W.A. (2021). Pedot:tosylate-polyamine-based organic electrochemical transistors for high-performance bioelectronics. *Adv. Electron. Mater.* 7, 2100059. <https://doi.org/10.1002/aelm.202100059>.
74. Li, W., Jin, J., Xiong, T., Yu, P., and Mao, L. (2022). Fast-scanning potential-gated organic electrochemical transistors for highly sensitive sensing of dopamine in living rat brain. *Angew. Chem., Int. Ed. Engl.* 61, e202204134. <https://doi.org/10.1002/anie.202204134>.
75. Xie, K., Wang, N., Lin, X., Wang, Z., Zhao, X., Fang, P., Yue, H., Kim, J., Luo, J., Cui, S., et al. (2020). Organic electrochemical transistor arrays for real-time mapping of evoked neurotransmitter release in vivo. *Elife* 9, e50345. <https://doi.org/10.7554/eLife.50345>.
76. Saraf, N., Woods, E.R., Peppler, M., and Seal, S. (2018). Highly selective aptamer based organic electrochemical biosensor with pico-level detection. *Biosens. Bioelectron.* 117, 40–46. <https://doi.org/10.1016/j.bios.2018.05.031>.
77. Song, J., Lin, P., Ruan, Y.F., Zhao, W.W., Wei, W., Hu, J., Ke, S., Zeng, X., Xu, J.J., Chen, H.Y., et al. (2018). Organic photo-electrochemical transistor-based biosensor: a proof-of-concept study toward highly sensitive dna detection. *Adv. Healthcare Mater.* 7, e1800536. <https://doi.org/10.1002/adhm.201800536>.
78. Sensi, M., Migatti, G., Beni, V., D'Alvise, T.M., Weil, T., Berto, M., Greco, P., Imbriano, C., Biscarini, F., and Bortolotti, C.A. (2022). Monitoring DNA hybridization with organic electrochemical transistors functionalized with polydopamine. *Macromol. Mater. Eng.* 307, 2100880. <https://doi.org/10.1002/mame.202100880>.
79. Gao, G., Hu, J., Li, Z., Xu, Q., Wang, C.-S., Jia, H.-M., Zhou, H., Lin, P., and Zhao, W.-W. (2022). Hybridization chain reaction for regulating surface capacitance of organic photoelectrochemical transistor toward sensitive miRNA detection. *Biosens. Bioelectron.* 209, 114224. <https://doi.org/10.1016/j.bios.2022.114224>.
80. Peng, J., He, T., Sun, Y., Liu, Y., Cao, Q., Wang, Q., and Tang, H. (2018). An organic electrochemical transistor for determination of microRNA21 using gold nanoparticles and a capture DNA probe. *Mikrochim. Acta* 185, 408–8. <https://doi.org/10.1007/s00604-018-2944-x>.
81. Fu, Y., Wang, N., Yang, A., Xu, Z., Zhang, W., Liu, H., Law, H.K.-w., and Yan, F. (2021). Ultrasensitive detection of ribonucleic acid biomarkers using portable sensing platforms based on organic electrochemical transistors. *Anal. Chem.* 93, 14359–14364. <https://doi.org/10.1021/acs.analchem.1c03441>.
82. Guo, K., Wustoni, S., Koklu, A., Díaz-Galicia, E., Moser, M., Hama, A., Alqahtani, A.A., Ahmad, A.N., Alhamlan, F.S., Shuaib, M., et al. (2021). Rapid single-molecule detection of COVID-19 and MERS antigens via nanobody-functionalized organic electrochemical transistors. *Nat. Biomed. Eng.* 5, 666–677. <https://doi.org/10.1038/s41551-021-00734-9>.
83. Liu, H., Yang, A., Song, J., Wang, N., Lam, P., Li, Y., Law, H.K.-w., and Yan, F. (2021). Ultrafast, sensitive, and portable detection of COVID-19 IgG using flexible organic electrochemical transistors. *Sci. Adv.* 7, eabg8387. <https://doi.org/10.1126/sciadv.abg8387>.
84. Li, Z., Hu, J., Gao, G., Liu, X.-N., Wu, J.-Q., Xu, Y.-T., Zhou, H., Zhao, W.-W., Xu, J.-J., and Chen, H.-Y. (2022). Organic photoelectrochemical transistor detection of tear lysozyme. *Sens. Diagn.* 1, 294–300. <https://doi.org/10.1039/D1SD00074H>.
85. Hu, J., Lu, M.J., Chen, F.Z., Jia, H.M., Zhou, H., Li, K., Zeng, X., Zhao, W.W., and Lin, P. (2022). Multifunctional hydrogel hybrid-gated organic photoelectrochemical transistor for biosensing. *Adv. Funct. Mater.* 32, 2109046. <https://doi.org/10.1002/adfm.202109046>.
86. Hai, W., Goda, T., Takeuchi, H., Yamaoka, S., Horiguchi, Y., Matsumoto, A., and Miyahara, Y. (2018). Human influenza virus detection using sialyllactose-functionalized organic electrochemical transistors. *Sens. Actuators, B* 260, 635–641. <https://doi.org/10.1016/j.snb.2018.01.081>.
87. Koklu, A., Wustoni, S., Guo, K., Silva, R., Salvigni, L., Hama, A., Diaz-Galicia, E., Moser, M., Marks, A., McCulloch, I., et al. (2022). Convection driven ultrarapid protein detection via nanobody-functionalized organic electrochemical transistors. *Adv. Mater.* 34, 2202972. <https://doi.org/10.1002/adma.202202972>.
88. Yu, J., Yang, A., Wang, N., Ling, H., Song, J., Chen, X., Lian, Y., Zhang, Z., Yan, F., and Gu, M. (2021). Highly sensitive detection of caspase-3 activity based on peptide-modified organic electrochemical transistor biosensors. *Nanoscale* 13, 2868–2874. <https://doi.org/10.1039/d0nr08453k>.
89. Zhang, L., Wang, G., Xiong, C., Zheng, L., He, J., Ding, Y., Lu, H., Zhang, G., Cho, K., and Qiu, L. (2018). Chirality detection of amino acid enantiomers by organic electrochemical

- transistor. *Biosens. Bioelectron.* 105, 121–128. <https://doi.org/10.1016/j.bios.2018.01.035>.
90. Koklu, A., Wustoni, S., Musteata, V.E., Ohayon, D., Moser, M., McCulloch, I., Nunes, S.P., and Inal, S. (2021). Microfluidic integrated organic electrochemical transistor with a nanoporous membrane for amyloid-beta detection. *ACS Nano* 15, 8130–8141. <https://doi.org/10.1021/acsnano.0c09893>.
91. Song, Y., Zhang, H., Mukhopadhyaya, T., Hall, A.S., and Katz, H.E. (2022). Sensitive organic electrochemical transistor biosensors: Comparing single and dual gate functionalization and different COOH-functionalized bioreceptor layers. *Biosens. Bioelectron.* 216, 114691. <https://doi.org/10.1016/j.bios.2022.114691>.
92. Song, Y., Lamberty, Z.D., Liang, J., Aller, Pellitero, M., Wagner, J.S., Juma'an, E., Bevan, M.A., Frechette, J., Arroyo-Currás, N., and Katz, H.E. (2021). Nanoscale bioreceptor layers comprising carboxylated polythiophene for organic electrochemical transistor-based biosensors. *ACS Appl. Nano Mater.* 4, 13459–13468. <https://doi.org/10.1021/acsnm.1c02949>.
93. He, R.-X., Zhang, M., Tan, F., Leung, P.H.M., Zhao, X.-Z., Chan, H.L.W., Yang, M., and Yan, F. (2012). Detection of bacteria with organic electrochemical transistors. *J. Mater. Chem.* 22, 22072–22076. <https://doi.org/10.1039/C2JM33667G>.
94. Tseng, A.C., and Sakata, T. (2022). Direct electrochemical signaling in organic electrochemical transistors comprising high-conductivity double-network hydrogels. *ACS Appl. Mater. Interfaces* 14, 24729–24740. <https://doi.org/10.1021/acsnami.2c01779>.
95. Yao, C., Xie, C., Lin, P., Yan, F., Huang, P., and Hsing, I.M. (2013). Organic electrochemical transistor array for recording transepithelial ion transport of human airway epithelial cells. *Adv. Mater.* 25, 6575–6580. <https://doi.org/10.1002/adma.201302615>.
96. Lin, P., Yan, F., Yu, J., Chan, H.L.W., and Yang, M. (2010). The application of organic electrochemical transistors in cell-based biosensors. *Adv. Mater.* 22, 3655–3660. <https://doi.org/10.1002/adma.201000971>.
97. Lin, P., Luo, X., Hsing, I.M., and Yan, F. (2011). Organic electrochemical transistors integrated in flexible microfluidic systems and used for label-free DNA sensing. *Adv. Mater.* 23, 4035–4040. <https://doi.org/10.1002/adma.201102017>.
98. Bidinger, S.L., Keene, S.T., Han, S., Plaxco, K.W., Malliaras, G.G., and Hasan, T. (2022). Pulsed transistor operation enables miniaturization of electrochemical aptamer-based sensors. *Sci. Adv.* 8, eadd4111. <https://doi.org/10.1126/sciadv.add4111>.
99. Fu, Y., Wang, N., Yang, A., Law, H.K.w., Li, L., and Yan, F. (2017). Highly sensitive detection of protein biomarkers with organic electrochemical transistors. *Adv. Mater.* 29, 1703787. <https://doi.org/10.1002/adma.201703787>.
100. Liao, C., Mak, C., Zhang, M., Chan, H.L.W., and Yan, F. (2015). Flexible organic electrochemical transistors for highly selective enzyme biosensors and used for saliva testing. *Adv. Mater.* 27, 676–681. <https://doi.org/10.1002/adma.201404378V>.
101. Tang, H., Yan, F., Lin, P., Xu, J., and Chan, H.L.W. (2011). Highly sensitive glucose biosensors based on organic electrochemical transistors using platinum gate electrodes modified with enzyme and nanomaterials. *Adv. Funct. Mater.* 21, 2264–2272. <https://doi.org/10.1002/adfm.201002117>.
102. Pappa, A.M., Curto, V.F., Braendlein, M., Strakosas, X., Donahue, M.J., Focchi, M., Malliaras, G.G., and Owens, R.M. (2016). Organic transistor arrays integrated with finger-powered microfluidics for multianalyte saliva testing. *Adv. Healthcare Mater.* 5, 2295–2302. <https://doi.org/10.1002/adhm.201600494>.
103. Liao, C., Zhang, M., Niu, L., Zheng, Z., and Yan, F. (2013). Highly selective and sensitive glucose sensors based on organic electrochemical transistors with graphene-modified gate electrodes. *J. Mater. Chem. B* 1, 3820–3829. <https://doi.org/10.1039/C3TB20451K>.
104. Khodagholy, D., Curto, V.F., Fraser, K.J., Gurfinkel, M., Byrne, R., Diamond, D., Malliaras, G.G., Benito-Lopez, F., and Owens, R.M. (2012). Organic electrochemical transistor incorporating an ionogel as a solid state electrolyte for lactate sensing. *J. Mater. Chem.* 22, 4440–4443. <https://doi.org/10.1039/C2JM15716K>.
105. Scheiblin, G., Aliane, A., Strakosas, X., Curto, V.F., Coppard, R., Marchand, G., Owens, R.M., Mailley, P., and Malliaras, G.G. (2015). Screen-printed organic electrochemical transistors for metabolite sensing. *MRS Commun.* 5, 507–511. <https://doi.org/10.1557/mrc.2015.52>.
106. Zhang, S., Li, Y., Tomasello, G., Anthonisen, M., Li, X., Mazzeo, M., Genco, A., Grutter, P., and Cicoira, F. (2019). Tuning the electromechanical properties of PEDOT:PSS films for stretchable transistors and pressure sensors. *Adv. Electron. Mater.* 5, 1900191. <https://doi.org/10.1002/aeml.201900191>.
107. Chow, P.C.Y., and Someya, T. (2020). Organic photodetectors for next-generation wearable electronics. *Adv. Mater.* 32, 1902045. <https://doi.org/10.1002/adma.201902045>.
108. Zhong, Y., Koklu, A., Villalva, D.R., Zhang, Y., Hernandez, L.H., Moser, M., Hallani, R.K., McCulloch, I., Baran, D., and Inal, S. (2023). An organic electrochemical transistor integrated photodetector for high quality photoplethysmogram signal acquisition. *Adv. Funct. Mater.* 33, 2211479. <https://doi.org/10.1002/adfm.202211479>.
109. Campana, A., Cramer, T., Simon, D.T., Berggren, M., and Biscarini, F. (2014). Electrocardiographic recording with conformable organic electrochemical transistor fabricated on resorbable bioscaffold. *Adv. Mater.* 26, 3874–3878. <https://doi.org/10.1002/adma.201400263>.
110. Lee, W., Kim, D., Rivnay, J., Matsuhisa, N., Lonjaret, T., Yokota, T., Yawo, H., Sekino, M., Malliaras, G.G., and Someya, T. (2016). Integration of organic electrochemical and field-effect transistors for ultraflexible, high temporal resolution electrophysiology arrays. *Adv. Mater.* 28, 9722–9728. <https://doi.org/10.1002/adma.201602237>.
111. Noachtar, S., and Rémi, J. (2009). The role of EEG in epilepsy: a critical review. *Epilepsy Behav.* 15, 22–33. <https://doi.org/10.1016/j.yebeh.2009.02.035>.
112. Rivnay, J., Leleux, P., Ferro, M., Sessolo, M., Williamson, A., Koutsouras, D.A., Khodagholy, D., Ramuz, M., Strakosas, X., Owens, R.M., et al. (2015). High-performance transistors for bioelectronics through tuning of channel thickness. *Sci. Adv.* 1, e1400251. <https://doi.org/10.1126/sciadv.1400251>.
113. Khodagholy, D., Doublet, T., Quilichini, P., Gurfinkel, M., Leleux, P., Ghestem, A., Ismailova, E., Hervé, T., Sanaur, S., Bernard, C., and Malliaras, G.G. (2013). In vivo recordings of brain activity using organic transistors. *Nat. Commun.* 4, 1575–1577. <https://doi.org/10.1038/ncomms2573>.
114. Sugiyama, M., Uemura, T., Kondo, M., Akiyama, M., Namba, N., Yoshimoto, S., Noda, Y., Araki, T., and Sekitani, T. (2019). An ultraflexible organic differential amplifier for recording electrocardiograms. *Nat. Electron.* 2, 351–360. <https://doi.org/10.1038/s41928-019-0283-5>.
115. Luo, Z., Peng, B., Zeng, J., Yu, Z., Zhao, Y., Xie, J., Lan, R., Ma, Z., Pan, L., Cao, K., et al. (2021). Sub-thermionic, ultra-high-gain organic transistors and circuits. *Nat. Commun.* 12, 1928–1929. <https://doi.org/10.1038/s41467-021-22192-2>.
116. Zhang, Y., Li, J., Li, R., Sbircea, D.-T., Giovannitti, A., Xu, J., Xu, H., Zhou, G., Bian, L., McCulloch, I., and Zhao, N. (2017). Liquid-solid dual-gate organic transistors with tunable threshold voltage for cell sensing. *ACS Appl. Mater. Interfaces* 9, 38687–38694. <https://doi.org/10.1021/acsnami.7b09384>.
117. Gu, X., Yao, C., Liu, Y., and Hsing, I.M. (2016). 16-Channel organic electrochemical transistor array for in vitro conduction mapping of cardiac action potential. *Adv. Healthcare Mater.* 5, 2345–2351. <https://doi.org/10.1002/adhm.201600189>.
118. Strakosas, X., Sessolo, M., Hama, A., Rivnay, J., Stavrinidou, E., Malliaras, G.G., and Owens, R.M. (2014). A facile biofunctionalisation route for solution processable conducting polymer devices. *J. Mater. Chem. B* 2, 2537–2545. <https://doi.org/10.1039/C3TB21491E>.
119. Sessolo, M., Rivnay, J., Bandiello, E., Malliaras, G.G., and Bolink, H.J. (2014). Ion-selective organic electrochemical transistors. *Adv. Mater.* 26, 4803–4807. <https://doi.org/10.1002/adma.201400731>.
120. Scheiblin, G., Coppard, R., Owens, R.M., Mailley, P., and Malliaras, G.G. (2017). Referenceless pH sensor using organic electrochemical transistors. *Adv. Mater. Technol.* 2, 1600141. <https://doi.org/10.1002/admt.201600141>.
121. Demuru, S., Kunnell, B.P., and Briand, D. (2020). Real-time multi-ion detection in the sweat concentration range enabled by flexible, printed, and microfluidics-integrated organic transistor arrays. *Adv. Mater. Technol.*

- 5, 2000328. <https://doi.org/10.1002/admt.202000328>.
122. Feng, J., Fang, Y., Wang, C., Chen, C., Tang, C., Guo, Y., Wang, L., Yang, Y., Zhang, K., Wang, J., et al. (2023). All-Polymer Fiber Organic Electrochemical Transistor for Chronic Chemical Detection in the Brain. *Adv. Funct. Mater.* 33, 2214945. <https://doi.org/10.1002/adfm.202214945>.
123. Fang, Y., Feng, J., Shi, X., Yang, Y., Wang, J., Sun, X., Li, W., Sun, X., and Peng, H. (2023). Coaxial fiber organic electrochemical transistor with high transconductance. *Nano Res.* 16, 11885–11892. <https://doi.org/10.1007/s12274-023-5722-y>.
124. Warburg, O. (1956). On the origin of cancer cells. *Science* 123, 309–314. <https://doi.org/10.1126/science.123.3191.309>.
125. Braendlein, M., Pappa, A.M., Ferro, M., Lopresti, A., Acquaviva, C., Mamessier, E., Malliaras, G.G., and Owens, R.M. (2017). Lactate detection in tumor cell cultures using organic transistor circuits. *Adv. Mater.* 29, 1605744. <https://doi.org/10.1002/adma.201605744>.
126. Li, M., Yin, F., Song, L., Mao, X., Li, F., Fan, C., Zuo, X., and Xia, Q. (2021). Nucleic acid tests for clinical translation. *Chem. Rev.* 121, 10469–10558. <https://doi.org/10.1021/acs.chemrev.1c00241>.
127. Casalini, S., Bortolotti, C.A., Leonardi, F., and Biscarini, F. (2017). Self-assembled monolayers in organic electronics. *Chem. Soc. Rev.* 46, 40–71. <https://doi.org/10.1039/C6CS00509H>.
128. Gao, G., Chen, J.-H., Li, C.-J., Wang, C.-S., Hu, J., Zhou, H., Lin, P., Xu, Q., and Zhao, W.-W. (2022). Duplex-specific nuclease-enabled target recycling on semiconducting metal–organic framework heterojunctions for energy-transfer-based organic photoelectrochemical transistor mirna biosensing. *Anal. Chem.* 94, 15856–15863. <https://doi.org/10.1021/acs.analchem.2c03859>.
129. Ban, R., Lu, M.-J., Hu, J., Li, C.-J., Li, Y.-M., Gao, G., Wang, C.-S., Kong, F.-Y., Zhou, H., Lin, P., and Zhao, W.-W. (2022). Biological modulating organic photoelectrochemical transistor through in situ enzymatic engineering of photoactive gate for sensitive detection of serum alkaline phosphatase. *Biosens. Bioelectron.* 218, 114752. <https://doi.org/10.1016/j.bios.2022.114752>.
130. Li, Z., Xu, Y.-T., Hu, J., Wang, T., Liu, F.-Q., Zhou, H., Chen, G.-X., Lin, P., Zhao, W.-W., Xu, J.-J., and Chen, H.-Y. (2023). High-gain signal on PEDOT:PSS organic photoelectrochemical transistor biosensing modulated by a MXene/MOFs/NiO Schottky heterojunction. *Sci. China Chem.* 66, 578–585. <https://doi.org/10.1007/s11426-022-1425-9>.
131. Qu, P., Li, C.-J., Hu, J., Gao, G., Lin, P., and Zhao, W.-W. (2023). Hybridization chain reaction-enhanced biocatalytic precipitation on flower-like bi2s3: toward organic photoelectrochemical transistor aptasensing with high transconductance. *Anal. Chem.* 95, 9983–9989. <https://doi.org/10.1021/acs.analchem.3c01185>.
132. Harikesh, P.C., Yang, C.Y., Tu, D., Gerasimov, J.Y., Dar, A.M., Armada-Moreira, A., Massetti, M., Kroon, R., Bliman, D., Olsson, R., et al. (2022). Organic electrochemical neurons and synapses with ion mediated spiking. *Nat. Commun.* 13, 901. <https://doi.org/10.1038/s41467-022-28483-6>.
133. Nawaz, A., Liu, Q., Leong, W.L., Fairfull-Smith, K.E., and Sonar, P. (2021). Organic Electrochemical Transistors for In Vivo Bioelectronics. *Adv. Mater.* 33, 2101874. <https://doi.org/10.1002/adma.202101874>.
134. Zhou, X., Zhang, L., Wang, Y., Zhao, S., Zhou, Y., Guo, Y., Wang, Y., Liang, J., and Chen, H. (2023). Aerosol jet printing of multi-dimensional oect force sensor with high sensitivity and large measuring range. *Adv. Mater. Technol.* 8, 2201272. <https://doi.org/10.1002/admt.202201272>.
135. Ho, V.M., Lee, J.-A., and Martin, K.C. (2011). The cell biology of synaptic plasticity. *Science* 334, 623–628. <https://doi.org/10.1126/science.1209236>.
136. van De Burgt, Y., Melianas, A., Keene, S.T., Malliaras, G., and Salleo, A. (2018). Organic electronics for neuromorphic computing. *Nat. Electron.* 1, 386–397. <https://doi.org/10.1038/s41928-018-0103-3>.
137. Kim, Y., Chortos, A., Xu, W., Liu, Y., Oh, J.Y., Son, D., Kang, J., Foudeh, A.M., Zhu, C., Lee, Y., et al. (2018). A bioinspired flexible organic artificial afferent nerve. *Science* 360, 998–1003. <https://doi.org/10.1126/science.aao0098>.
138. Deng, Y., Zhao, M., Ma, Y., Liu, S., Liu, M., Shen, B., Li, R., Ding, H., Cheng, H., Sheng, X., et al. (2023). A flexible and biomimetic olfactory synapse with gasotransmitter-mediated plasticity. *Adv. Funct. Mater.* 33, 2214139. <https://doi.org/10.1002/adfm.202214139>.
139. Bartolozzi, C., Natale, L., Nori, F., and Metta, G. (2016). Robots with a sense of touch. *Nat. Mater.* 15, 921–925. <https://doi.org/10.1038/nmat4731>.
140. Shim, H., Ershad, F., Patel, S., Zhang, Y., Wang, B., Chen, Z., Marks, T.J., Facchetti, A., and Yu, C. (2022). An elastic and reconfigurable synaptic transistor based on a stretchable bilayer semiconductor. *Nat. Electron.* 5, 660–671. <https://doi.org/10.1038/s41928-022-00859-y>.
141. Shim, H., Sim, K., Ershad, F., Yang, P., Thukral, A., Rao, Z., Kim, H.-J., Liu, Y., Wang, X., Gu, G., et al. (2019). Stretchable elastic synaptic transistors for neurologically integrated soft engineering systems. *Sci. Adv.* 5, eaax4961. <https://doi.org/10.1126/sciadv.aax4961>.
142. Jang, S., Jang, S., Lee, E.-H., Kang, M., Wang, G., and Kim, T.-W. (2019). Ultrathin conformable organic artificial synapse for wearable intelligent device applications. *ACS Appl. Mater. Interfaces* 11, 1071–1080. <https://doi.org/10.1021/acsami.8b12092>.
143. Keene, S.T., Lubrano, C., Kazemzadeh, S., Melianas, A., Tuchman, Y., Polino, G., Scognamiglio, P., Cinà, L., Salleo, A., van de Burgt, Y., and Santoro, F. (2020). A biohybrid synapse with neurotransmitter-mediated plasticity. *Nat. Mater.* 19, 969–973. <https://doi.org/10.1038/s41563-020-0703-y>.
144. Lubrano, C., Bruno, U., Ausilio, C., and Santoro, F. (2022). Supported lipid bilayers coupled to organic neuromorphic devices modulate short-term plasticity in biomimetic synapses. *Adv. Mater.* 34, 2110194. <https://doi.org/10.1002/adma.202110194>.
145. Harikesh, P.C., Yang, C.-Y., Wu, H.-Y., Zhang, S., Donahue, M.J., Caravaca, A.S., Huang, J.-D., Olofsson, P.S., Berggren, M., Tu, D., and Fabiano, S. (2023). Ion-tunable antiambipolarity in mixed ion–electron conducting polymers enables biorealistic organic electrochemical neurons. *Nat. Mater.* 22, 242–248. <https://doi.org/10.1038/s41563-022-01450-8>.
146. Sarkar, T., Lieberth, K., Pavlou, A., Frank, T., Mailaender, V., McCulloch, I., Blom, P.W.M., Torricelli, F., and Gkoupidenis, P. (2022). An organic artificial spiking neuron for in situ neuromorphic sensing and biointerfacing. *Nat. Electron.* 5, 774–783. <https://doi.org/10.1038/s41928-022-00859-y>.
147. Kim, S.J., Jeong, J.S., Jang, H.W., Yi, H., Yang, H., Ju, H., and Lim, J.A. (2021). Dendritic network implementable organic neurofiber transistors with enhanced memory cyclic endurance for spatiotemporal iterative learning. *Adv. Mater.* 33, 2100475. <https://doi.org/10.1002/adma.202100475>.
148. Gkoupidenis, P., Schaefer, N., Garlan, B., and Malliaras, G.G. (2015). Neuromorphic functions in PEDOT:PSS organic electrochemical transistors. *Adv. Mater.* 27, 7176–7180. <https://doi.org/10.1002/adma.201503674>.
149. Lee, Y.R., Trung, T.Q., Hwang, B.-U., and Lee, N.-E. (2020). A flexible artificial intrinsic-synaptic tactile sensory organ. *Nat. Commun.* 11, 2753. <https://doi.org/10.1038/s41467-020-16606-w>.
150. Liu, D., Tian, X., Bai, J., Wang, Y., Cheng, Y., Ning, W., Chan, P.K.L., Wu, K., Sun, J., and Zhang, S. (2022). Intrinsically stretchable organic electrochemical transistors with rigid-device-benchmarkable performance. *Adv. Sci.* 9, 2203418. <https://doi.org/10.1002/advs.202203418>.
151. Su, X., Wu, X., Chen, S., Nedumaran, A.M., Stephen, M., Hou, K., Czarny, B., and Leong, W.L. (2022). A highly conducting polymer for self-healable, printable, and stretchable organic electrochemical transistor arrays and near hysteresis-free soft tactile sensors. *Adv. Mater.* 34, 2200682. <https://doi.org/10.1002/adma.202200682>.
152. Boutry, C.M., Negre, M., Jorda, M., Vardoulis, O., Chortos, A., Khatib, O., and Bao, Z. (2018). A hierarchically patterned, bioinspired e-skin able to detect the direction of applied pressure for robotics. *Sci. Robot.* 3, eaau6914. <https://doi.org/10.1126/scirobotics.aau6914>.
153. Stavrinidou, E., Gabrielsson, R., Gomez, E., Crispin, X., Nilsson, O., Simon, D.T., and Berggren, M. (2015). Electronic plants. *Sci. Adv.* 1, e1501136. <https://doi.org/10.1126/sciadv.1501136>.
154. Janni, M., Coppede, N., Bettelli, M., Briglia, N., Petrozza, A., Summerer, S., Vurro, F., Danzi, D., Cellini, F., Marmiroli, N., et al. (2019). In Vivo Phenotyping for the Early

- Detection of Drought Stress in Tomato. *Plant Phenomics* 2019. <https://doi.org/10.34133/2019/6168209>.
155. Gentile, F., Vurro, F., Janni, M., Manfredi, R., Cellini, F., Petrozza, A., Zappettini, A., and Coppedè, N. (2022). A Biomimetic, Biocompatible OECT Sensor for the Real-Time Measurement of Concentration and Saturation of Ions in Plant Sap. *Adv. Electron. Mater.* 8, 2200092. <https://doi.org/10.1002/aelm.202200092>.
 156. Coppedè, N., Janni, M., Bettelli, M., Maida, C.L., Gentile, F., Villani, M., Ruotolo, R., Iannotta, S., Marmioli, N., Marmioli, M., and Zappettini, A. (2017). An in vivo biosensing, biomimetic electrochemical transistor with applications in plant science and precision farming. *Sci. Rep.* 7, 16195. <https://doi.org/10.1038/s41598-017-16217-4>.
 157. Diacci, C., Abedi, T., Lee, J.W., Gabrielson, E.O., Berggren, M., Simon, D.T., Niittylä, T., and Stavriniidou, E. (2021). Diurnal in vivo xylem sap glucose and sucrose monitoring using implantable organic electrochemical transistor sensors. *iScience* 24, 101966. <https://doi.org/10.1016/j.isci.2020.101966>.
 158. Bischak, C.G., Flagg, L.Q., and Ginger, D.S. (2020). Ion Exchange Gels Allow Organic Electrochemical Transistor Operation with Hydrophobic Polymers in Aqueous Solution. *Adv. Mater.* 32, 2002610. <https://doi.org/10.1002/adma.202002610>.
 159. Strand, E.J., Bihar, E., Gleason, S.M., Han, S., Schreiber, S.W., Renny, M.N., Malliaras, G.G., McLeod, R.R., and Whiting, G.L. (2022). Printed Organic Electrochemical Transistors for Detecting Nutrients in Whole Plant Sap. *Adv. Electron. Mater.* 8, 2100853. <https://doi.org/10.1002/aelm.202100853>.
 160. Song, Y., Min, J., Yu, Y., Wang, H., Yang, Y., Zhang, H., and Gao, W. (2020). Wireless battery-free wearable sweat sensor powered by human motion. *Sci. Adv.* 6, eaay9842. <https://doi.org/10.1126/sciadv.aay9842>.
 161. Gao, W., Emaminejad, S., Nyein, H.Y.Y., Challa, S., Chen, K., Peck, A., Fahad, H.M., Ota, H., Shiraki, H., Kiriya, D., et al. (2016). Fully integrated wearable sensor arrays for multiplexed in situ perspiration analysis. *Nature* 529, 509–514. <https://doi.org/10.1038/nature16521>.
 162. Jiang, Y., Zhang, Z., Wang, Y.-X., Li, D., Coen, C.-T., Hwaun, E., Chen, G., Wu, H.-C., Zhong, D., Niu, S., et al. (2022). Topological supramolecular network enabled high-conductivity, stretchable organic bioelectronics. *Science* 375, 1411–1417. <https://doi.org/10.1126/science.abj7564>.
 163. Min, J., Demchysyn, S., Sempionatto, J.R., Song, Y., Hailegnaw, B., Xu, C., Yang, Y., Solomon, S., Putz, C., Lehner, L.E., et al. (2023). An autonomous wearable biosensor powered by a perovskite solar cell. *Nat. Electron.* 6, 630–641. <https://doi.org/10.1038/s41928-023-00996-y>.
 164. Waltz, E. (2016). A spark at the periphery. *Nat. Biotechnol.* 34, 904–908. <https://doi.org/10.1038/nbt.3667>.